

## Passive regulation of soil biogeochemical cycling by root water transport

Juan C. Quijano,<sup>1</sup> Praveen Kumar,<sup>1</sup> and Darren T. Drewry<sup>2,3</sup>

Received 8 February 2013; revised 3 May 2013; accepted 13 May 2013; published 21 June 2013.

[2] Surface and subsurface moisture dynamics are strongly influenced by the ability of vegetation to take up and redistribute soil moisture using hydraulic redistribution (HR). These dynamics in turn affect soil biogeochemical cycling through controls on decomposition and mineralization rates and ion transport. The goal of this study is to explore this coupling between HR and biogeochemistry using a numerical model. We examine decomposition and mineralization of organic matter and analyze whether differences in decomposition rates induced by HR influence the long-term storage of carbon in the soil and the movement of nitrate ( $\text{NO}_3^-$ ) and ammonium ( $\text{NH}_4^+$ ) in the rhizosphere. These dynamics are studied in a framework that incorporates the interaction between multiple plant species. The net effect of HR on decomposition is controlled by a trade-off between the resultant moisture and temperature states. This trade-off is conditioned by the availability of fine roots near the surface, and it impacts the long-term storage and vertical distribution of carbon in the soil. HR also impacts the transport and uptake of ions from the soil. It reduces the leaching of nitrate considerably, and, therefore facilitates the uptake of nitrate by vegetation roots. Furthermore, the magnitude and patterns of the feedbacks induced by HR are also influenced by the presence of different plant species that coexist. These results suggest that the alteration of soil moisture by plants through associated processes such as HR can have considerable impact on the below-ground biogeochemical cycling of carbon and nitrogen.

**Citation:** Quijano, J. C., P. Kumar, and D. T. Drewry (2013), Passive regulation of soil biogeochemical cycling by root water transport, *Water Resour. Res.*, 49, 3729–3746, doi:10.1002/wrcr.20310.

### 1. Introduction

[3] Plant root systems provide the pathway for moisture uptake required by above-ground vegetation and therefore are a critical component of the terrestrial hydrologic cycle. In addition to water uptake, the ability of plant roots to passively transport moisture throughout the soil column following water potential gradients has been widely observed and is generally referred to as *hydraulic redistribution* (HR) [Burgess *et al.*, 1998, 2000, 2001; Amenu and Kumar, 2008; Quijano *et al.*, 2012]. Three main types of redistribution have been observed: (i) hydraulic lift (HL) where water is transported upward from wet deep to dry shallow layers [Dawson, 1993; Espeleta *et al.*, 2004; Ishikawa and Bledsoe, 2000; Ludwig *et al.*, 2003], (ii) hydraulic

descent (HD) where water is transported downward from shallow wet layers to deep dry layers [Burgess *et al.*, 1998; Schulze *et al.*, 1998; Smith *et al.*, 1999; Hultine *et al.*, 2003], and (iii) lateral redistribution (LD) where water is transported horizontally from patches of wet to dry soil [Brooks *et al.*, 2002, 2006; Nadezhkina *et al.*, 2010]. The importance of characteristics such as root biomass distribution and associated processes such as HR in subsurface moisture dynamics have led to several studies that have analyzed the role of plant roots in regulating soil-moisture patterns and associated impacts on vegetation water and energy balances as well as ecosystem productivity [Ryel *et al.*, 2002; Brooks *et al.*, 2002; Amenu and Kumar, 2008; Scott *et al.*, 2008; Quijano *et al.*, 2012]. However, the potential influence of HR on below-ground biogeochemical cycling of carbon and nitrogen has been suggested [Caldwell and Richards, 1989; Caldwell *et al.*, 1998; Horton and Hart, 1998; Dawson, 1993; Jackson *et al.*, 2000; Hawkins *et al.*, 2009; Liste and White, 2008; Richards and Caldwell, 1987] and is the focus of the present work using a modeling approach.

[4] Water uptake and HR regulate the distribution of soil-moisture at the ground surface, influencing the release of latent heat from the soil (soil evaporation) [Quijano *et al.*, 2012], and the surface energy balance. As a result, the input of heat into the ground and the near-surface soil temperature is also regulated by root water transport. Soil moisture and temperature affect the biochemical reactions

Additional supporting information may be found in the online version of this article.

<sup>1</sup>Department of Civil and Environmental Engineering, University of Illinois at Urbana Champaign, Urbana, Illinois, USA.

<sup>2</sup>Max Planck Institute for Biogeochemistry, Jena, Germany.

<sup>3</sup>Now at Jet Propulsion Laboratory, Pasadena, California, USA.

Corresponding author: P. Kumar, Department of Civil and Environmental Engineering, University of Illinois at Urbana Champaign, Hydrosystems Building, Urbana, IL 61802, USA. (kumar1@illinois.edu)

©2013. American Geophysical Union. All Rights Reserved.  
0043-1397/13/10.1002/wrcr.20310

and microbial activity in the soil [Kieft *et al.*, 1993; Zogg *et al.*, 1997; Lundquist *et al.*, 1999; Sylvia *et al.*, 2005], thereby influencing processes such as decomposition of organic matter and nutrient mineralization [Kätterer *et al.*, 1998; Manzoni and Porporato, 2009]. On the other hand, the availability of soil moisture impacts the transport of ions in the subsurface. Higher soil moisture enhances diffusion of ions in the soil [Nye and Tinker, 1977; Caldwell and Manwaring, 1994], and soil moisture fluxes induced by gradients in water potential can carry soluble ions such as nitrate ( $\text{NO}_3^-$ ) and dissolved organic carbon. Furthermore, the redistribution of moisture to dry layers can increase the lifespan of fine roots [Caldwell *et al.*, 1998; Matzner and Richards, 1996], extending the period of plant nutrient uptake during dry seasons.

[5] The study of *de Kroon et al.* [1998] observed  $\text{NO}_3^-$  translocation by the root systems of *Carex flacca*. Nitrate translocation was more prominent where the  $\text{NO}_3^-$  concentration gradient and water potential gradient were in the same direction. McCulley *et al.* [2004] observed a high availability of several nutrients (particularly P,  $\text{Ca}^{2+}$ ,  $\text{Mg}^{2+}$ ) at deeper layers, which explain the presence of deep roots in arid and semiarid ecosystems and propose HD as a mechanism that facilitates the formation of this pool. Aanderud and Richards [2009] studied the role of HR in decomposition rates in a field experiment with two different shrub species, *Artemisia* and *Sarcobatus*. They observed higher decomposition rates under the presence of HR. In a recent experiment with Buffalo grass, Armas *et al.* [2011] observed higher rates of organic matter decomposition and mineralization of nitrogen in the presence of HL. They also observed that the presence of HL enhanced plant nitrogen uptake.

[6] Other experimental studies have shown indirect influence of HR by its capacity to prolong root and microbial activity. Matzner and Richards [1996] ran an experiment with *Artemisia tridentata* to analyze the role of HL in enhancing phosphorus and nitrogen uptake. They found that HL plays an important role because it maintains higher levels of soil water potential, thereby enhancing root longevity. The influence of HL to increase root longevity during dry periods, together with the capacity of *A. tridentata* to uptake nutrients under low water potentials, allow this species to sustain a stable uptake of phosphorus and nitrogen during the dry period. Querejeta *et al.* [2003, 2007] and Egerton-Warburton *et al.* [2008] observed that the presence of HL enhances mycorrhiza fungi function during dry periods. Egerton-Warburton *et al.* [2008] observed that efflux of moisture through HL from mycorrhizal hyphae in seedlings of *Quercus agrifolia* enhanced soil processes such as bacterial growth and soil enzyme activity. In a field experiment with Ponderosa Pine, common mycorrhizal networks connecting different plants were found to transport HL water, enhancing the survival of shallow rooted plants during drought [Warren *et al.*, 2008].

[7] In this study, we use a detailed multispecies process-based numerical model of the coupled canopy-root-soil systems [Quijano *et al.*, 2012] to examine the interplay between HR and multiple plant species that coexist, and analyze how this interplay influence the carbon and nitrogen dynamics throughout the vertical soil column. Specifically, we address the following questions: (i) What is the influ-

ence of HR on soil organic matter decomposition and how does it influence the long-term concentration and distribution of carbon in the soil column? (ii) How does the presence of different plant species composition influence the impact of HR on the carbon dynamics? (iii) What is the influence of HR on the long-term concentration, distribution, and fluxes of mineral nitrogen (nitrate  $\text{NO}_3^-$  and ammonium  $\text{NH}_4^+$ ) in the soil column? and (iv) How does the presence of multiple plant species composition alter the effect of HR on the nitrogen dynamics? A list of all symbols used is included in the online supporting information.

## 2. Methods

### 2.1. Model Formulation

[8] In order to capture the interactions between different plant species that coexist, we use a multispecies model presented in Quijano *et al.* [2012], which was an extension of the multilayer canopy-root-soil system model (MLCan) presented in Drewry *et al.* [2010a, 2010b]. In this study, we further extend this multispecies model to include carbon and nitrogen dynamics drawing upon and extending the framework initially proposed by Porporato *et al.* [2003] (see also [D'Odorico *et al.*, 2003; Manzoni and Porporato, 2007]). The multispecies model simulates the ecohydrological dynamics in the presence of several plant species that share common resources such as below-ground soil moisture or above-ground incident radiation. Coexisting species can have different ecophysiological and structural features that result in different abilities to exploit the common resource.

[9] Above ground, the model solves the longwave and shortwave radiation regimes for each layer of the canopy using a compound leaf area distribution (LAD). The compound LAD is computed as a linear sum of the LAD of each plant species in each layer. The absorbed radiation for each species is then computed as the fraction that species contributes to the compound LAD at each layer. The model then solves the energy balance for all the different canopy layers for each species independently as a function of this absorbed energy. Through this approach, the model is able to predict photosynthetic carbon uptake and latent and sensible heat exchange with the atmosphere for each of the species considered.

[10] Below the ground, each species can exploit different parts of the soil column as a function of their unique rooting depths and root biomass distributions. Hydraulic redistribution is represented using a coupled set of differential equations [Amenu and Kumar, 2008] that describes moisture flow through the root system as a function of uptake capacity and potential gradients in the coupled soil-plant system. This framework allows us to simulate the presence of different species sharing the same soil column, effectively allowing for competitive or mutualistic interactions. The model simulates the effect of dry conditions in water uptake and water release (HR) by reducing the radial conductivity of the root system. This reduction is simulated by the implementation of a fine root conductivity loss function (FRCL) (see online supporting information section 1). We believe that this model, therefore, provides an effective tool with which to analyze the hydrological controls on

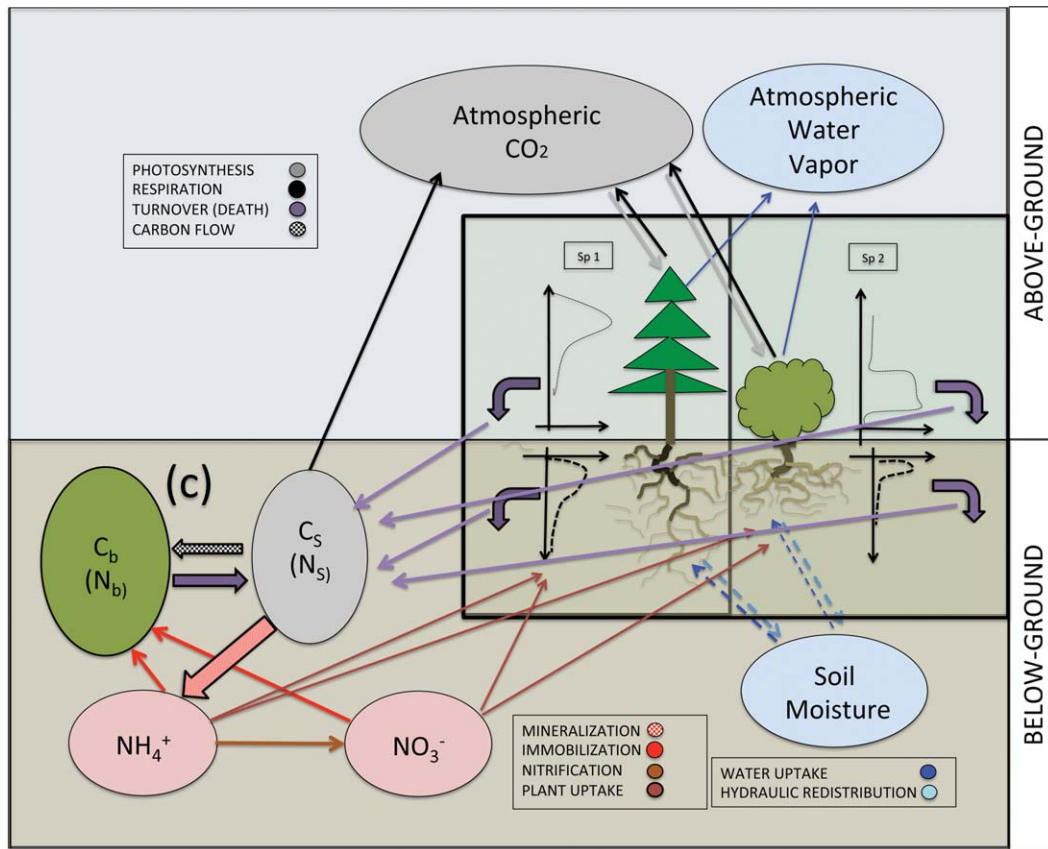


**Figure 1.** Schematic representation of the coupling between the multispecies MLCan model and the C:N model. Above ground, the radiative energy coming from the sun is absorbed by each species according to their leaf area distributions. In addition, each species has different ecophysiological properties resulting in distinct transpiration fluxes. Below the ground, the same pools of water and mineral nitrogen are shared by all the species. The uptake of water and mineral nitrogen in the soil is computed independently for each species as a function of the distribution of fine roots.

subsurface carbon and nitrogen dynamics when more than one species coexist and share resources.

[11] The C-N model simulates the main processes that control the carbon and nitrogen dynamics in the soil, such as decomposition, mineralization, immobilization, nitrification, water uptake, and leaching, using equations based on mass balance and C:N ratios [Porporato *et al.*, 2003; Manzoni and Porporato, 2007]. In this study, we extend this initial framework to include multiple soil layers, the effect of soil temperature on decomposition and the vertical flux of carbon from bioturbation. Figure 1 shows a schematic representation of this model, which includes the coupling between the multispecies MLCan and the C-N model. In this approach, roots from different plant species share both soil moisture and soil mineral nitrogen ( $NO_3^-$  and  $NH_4^+$ ) resources. This approach captures both facilitative and competitive interactions between plant species as influenced by HR.

[12] The bioturbation model allows for the transport of organic matter from the litter layer to horizon O and deeper horizons in the soil column. This is simulated using a diffusive process where the flux of organic carbon is proportional to the vertical carbon concentration gradient [Elzein and Balesdent, 1995; Dam *et al.*, 1997; Kaste *et al.*, 2007;

Braakhekke *et al.*, 2011]. Figure 1 in the online supporting information shows a schematic representation of the vertical carbon fluxes in the soil system, including bioturbation, and the model equations are given in the online supporting information (section 2).

## 2.2. Simulation Scenarios

[13] The simulations are run with data from Blodgett Forest Research Station and Blodgett Ameriflux site located in the Sierra Nevada near Georgetown, California. This site is characterized by wet winters and dry summers, typical of a Mediterranean climate. More details of site characteristics and Ameriflux data are presented in Quijano *et al.* [2012], Goldstein *et al.* [2000], Panek [2004], Fisher *et al.* [2005], Xu and Qi [2001], and Misson *et al.* [2004, 2006]. Although there is evidence that natural vegetation at this location is composed of a variety of understory and overstory species [Fisher *et al.*, 2005; Stephens and Mogg-haddas, 2005], for the simulations performed in this study we only consider the most dominant vegetation types: (i) *Pinus ponderosa* (hereafter PP) and (ii) understory shrubs (hereafter shrubs) that are composed of two dominant species *Arctostaphylos manzanita* (hereafter *Arctostaphylos*), and *Ceanothus cordulatus* (hereafter *Ceanothus*).

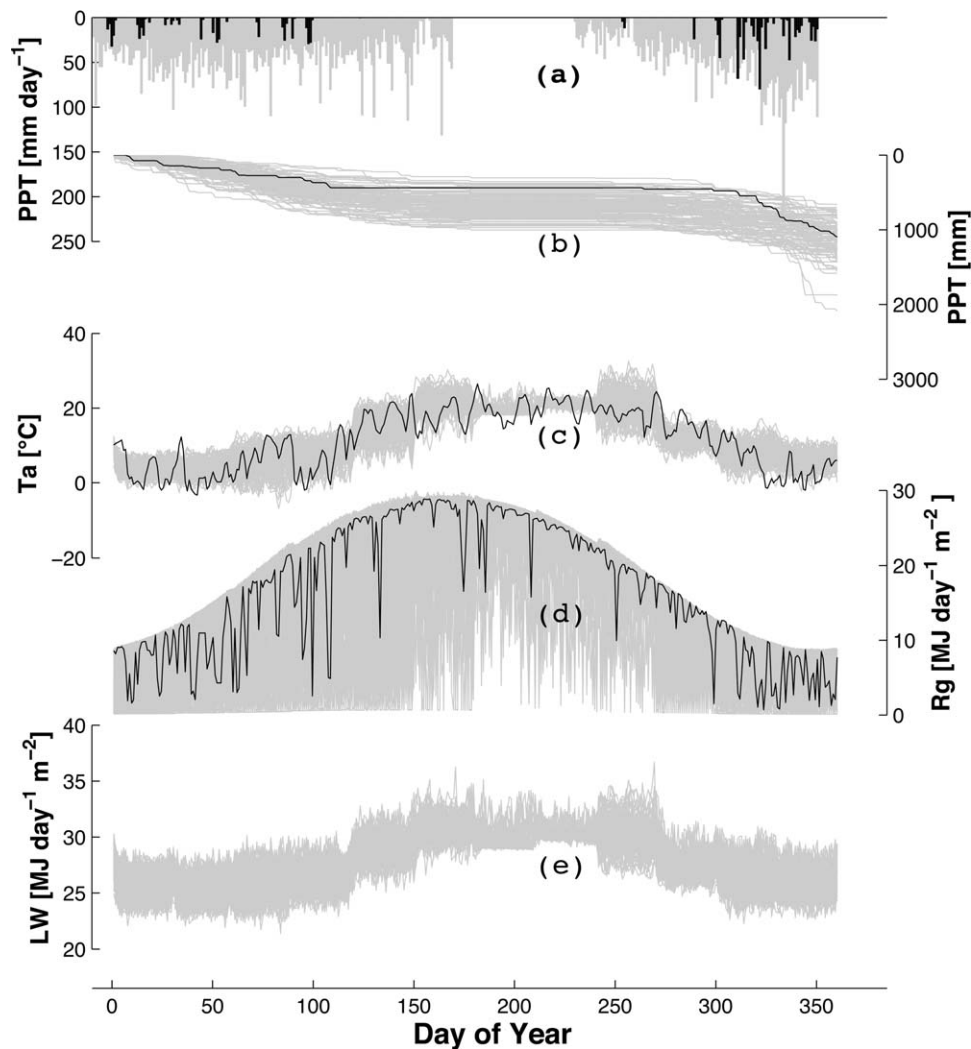


**Figure 2.** Annual time series of atmospheric variables used to force MLCan ecohydrological model used to conduct the simulations. Variables including (a) daily precipitation, (b) annual cumulated precipitation, (c) air temperature, (d) global radiation, and (e) incoming long-wave radiation were stochastically generated. Each figure displays an ensemble of 500 years of generated data. The realization in black corresponds to the observed variables at the Blodgett Ameriflux site in year 2001.

[14] To test the hypothesis that HR will result in differences in soil carbon and nitrogen cycling, and therefore modify the long-term accumulation of organic and mineral pools, we perform simulations for 500 years and analyze the equilibrium dynamics of soil hydrological and biogeochemical processes. The four different scenarios considered in this study are **(I)** presence of PP and shrubs with HR, **(II)** presence of PP and shrubs without HR, **(III)** presence of only PP with HR, and **(IV)** presence of only PP without HR.

### 2.3. Data Description

[15] Since Ameriflux data is available for only a limited period (2000–2006) and the carbon and nitrogen dynamics evolve over a much longer time scale, the forcing used in our study is derived from a stochastic weather generator [Ivanov *et al.*, 2007] parameterized using the observed Ameriflux data.

[16] Figure 2 shows the ensemble of 500 unique years of daily rainfall, annual cumulative rainfall, daily air tempera-

ture, daily global radiation, and daily incoming longwave radiation. The Mediterranean climate at this site is characterized by the out-of-phase rainfall and global radiation (also air temperature) throughout the year. The weather generation is performed for each year independently and does not consider interannual correlation. The same ensemble (and sequence) of atmospheric forcing (shown in Figure 2) is used for the simulations performed for all four scenarios.

[17] Other variables needed to run the model include plant species composition, leaf area index (LAI), foliage specific carbon leaf area index (SCLA), foliar C:N ratios, and ecohydrological parameters. These variables were assumed to exhibit the same intra-annual behavior for all the years of simulation. Within-year variability of these parameters was obtained from measurements made at the Blodgett Forest. In addition, we also assume that the soil structure (thickness of the different horizons) remains constant in time.



**Table 1.** Carbon and Nitrogen Model Parameters

Parameter	Symbol	Units	Value
Foliar parameters			
Needle lifespan PP		year	3
Leaf lifespan shrubs		year	3
Carbon-nitrogen dynamics			
Rate of nitrification	$k_n$	$\text{m}^3/\text{d}/\text{kgC}$	0.5
Fraction of decomposed organic matter going into respiration	$r_r$		0.7
Critical C:N above which immobilization occurs a	$(\text{C}:\text{N})_{\text{cr}}$ Fig 3		39.3
Microbial biomass C:N ratio	$(\text{C}:\text{N})_b$		11.8 <sup>b</sup>
Fraction of dissolved $\text{NH}_4^+$	$\lambda^+$		5
Fraction of dissolved $\text{NO}_3^-$	$\lambda^-$		100
Water potential below which microbial activity is water limited	$\psi_{\text{top}}$	MPa	-0.1 <sup>c</sup>
Water potential at which microbial activity is considered negligible	$\psi_{\text{min}}$	MPa	-10 <sup>c</sup>
Litter carbon concentration	$C_{s,\text{litter}}$	$\text{kg C m}^{-3}$	60 <sup>b,d</sup>
Litter thickness	$\Delta z_{\text{litter}}$	cm	3 <sup>d</sup>
Litter fragmentation parameter	$k_{\text{litter}}$	$\text{d}^{-1}$	$2.85 \times 10^{-7e}$
Leaves biomass and fine root biomass proportionally constant	$\text{km}_r$	–	0.8
Bioturbation diffusion constant at the surface	$D_b$	$\text{cm}^2/\text{year}$	4 <sup>f,g,h</sup>
Depth below which bioturbation is considered negligible	$z_{\text{biot}}$	cm	80
Total annual deposition	$N_{\text{dep}}$	$\text{g/yr}$	0.5
Root diffusion N uptake factor	$F_{\text{factor}}$	$\text{mm}/\text{d}/\text{kg}_{\text{root}}$	1.8

<sup>a</sup>Manzoni and Porporato [2007].<sup>b</sup>Bird and Torn [2006].<sup>c</sup>Andren [1992].<sup>d</sup>Black and Harden [1995].<sup>e</sup>Found by calibration.<sup>f</sup>Elzein and Balesdent [1995].<sup>g</sup>Dam et al. [1997].<sup>h</sup>Kaste et al. [2007].

[18] Table 1 displays a list of the most relevant parameters and the values implemented in this study. The details of the input data used in this model are briefly presented below.

### 2.3.1. LAI

[19] Figure 3a shows the seasonal dynamics of PP and shrub LAI. LAI was constructed using previous studies and available measurements that have been collected at the Blodgett site [Goldstein et al., 2000; Misson et al., 2007; Bouvier-Brown, 2008].

### 2.3.2. C:N Ratios

[20] The foliage C:N ratio varies seasonally throughout the year. Figure 3b shows the seasonal dynamics of the C:N ratio of the foliage for each species considered [Misson et al., 2007]. *Ceanothus* has the smallest C:N ratio because of its symbiotic fixation of nitrogen [Misson et al., 2007]. The C:N ratio in PP and *Arctostaphylos* are similar in magnitude but out of phase. The C:N ratio for *Arctostaphylos* and *Ceanothus* is weighted using the corresponding

LAI to calculate the net shrubs C:N ratio. We assume that the fine root C:N ratio is the same as that of the foliage. Figure 3b also shows the critical C:N ratio,  $(\text{C}:\text{N})_{\text{cr}}$ , which is the maximum C:N ratio required in the organic matter at which micro-organisms can sustain decomposition without immobilizing mineral nitrogen from the soil and is defined as the ratio between the C:N ratio in the microbial pool,  $(\text{C}:\text{N})_b$ , and the fraction of decomposed organic matter that goes into respiration,  $r_r$  ( $(\text{C}:\text{N})_{\text{cr}} = (\text{C}:\text{N})_b/r_r$ ) [Manzoni and Porporato, 2007]. It can be observed that for half of the year the foliage C:N ratio of PP is observed to be below  $(\text{C}:\text{N})_{\text{cr}}$ . However, the C:N in the soil is lower than the  $(\text{C}:\text{N})_{\text{cr}}$  for the entire year and, therefore, the system is under a net mineralization regime throughout the year.

### 2.3.3. Carbon Input

[21] Figure 3c shows the annual cumulative input of organic carbon to the soil from above-ground foliage deposition. These values are calculated using the available information on seasonal variation of LAI (Figure 3a), SCLA [Misson et al., 2006], and foliar C:N ratios in PP and shrubs (Figure 3b). The equations used to compute the above-ground loss of foliage are given in the online supporting information (section 3).

### 2.3.4. Soil Horizon Structure

[22] Black and Harden [1995] analyzed the organic matter composition and thickness of the litter layer and horizons O, A1, and A2 for ecosystems with different ages at the Blodgett Forest site. As expected the soil structure changes with time in Blodgett. The main difference is observed in the thickness of the litter layer and the thickness of the organic horizon. We use a representative structure with a litter layer of 4 cm and an organic horizon of 2 cm that are fixed in time. This structure represents an old growth ecosystem [Black and Harden, 1995].

### 2.3.5. Fine Roots Near the Surface

[23] The presence of fine roots in the near-surface zone is a critical variable that impacts the energy and water balance at the surface [Quijano et al., 2012]. Previous studies at Blodgett reported no evidence of fine roots in the litter layer and organic horizon [Walker et al., 2010]. Thus, in the simulations performed in this study, we assume absence of fine roots in either of these two layers. Walker et al. [2010] reported the presence of fine roots in horizon A at Blodgett. However, the dry conditions during the summer could trigger death of fine roots located in horizon A, which could be a mechanism to reduce the hydraulic conductivity with the soil and avoid the loss of water to soil evaporation [Espeleta et al., 2004; Quijano et al., 2012]. We simulate the response of fine roots to dry conditions using a function that considers the fine roots conductivity loss FRCL (Figure 3d, online supporting information, section 1). The same FRCL function was implemented for both PP and shrubs.

### 2.3.6. Initial Conditions for Carbon and Nitrogen Pools

[24] The initial concentrations of carbon in the organic matter pool ( $C_s$ ) and the microbial biomass pool ( $C_b$ ) were established according to available information observed and reconstructed in Blodgett Forest for the entire soil column (online supporting information section 4). Figure 4 shows the Blodgett Forest observations [Bird and Torn, 2006; Black and Harden, 1995] and the profiles reconstructed using an exponential model for vertical variation

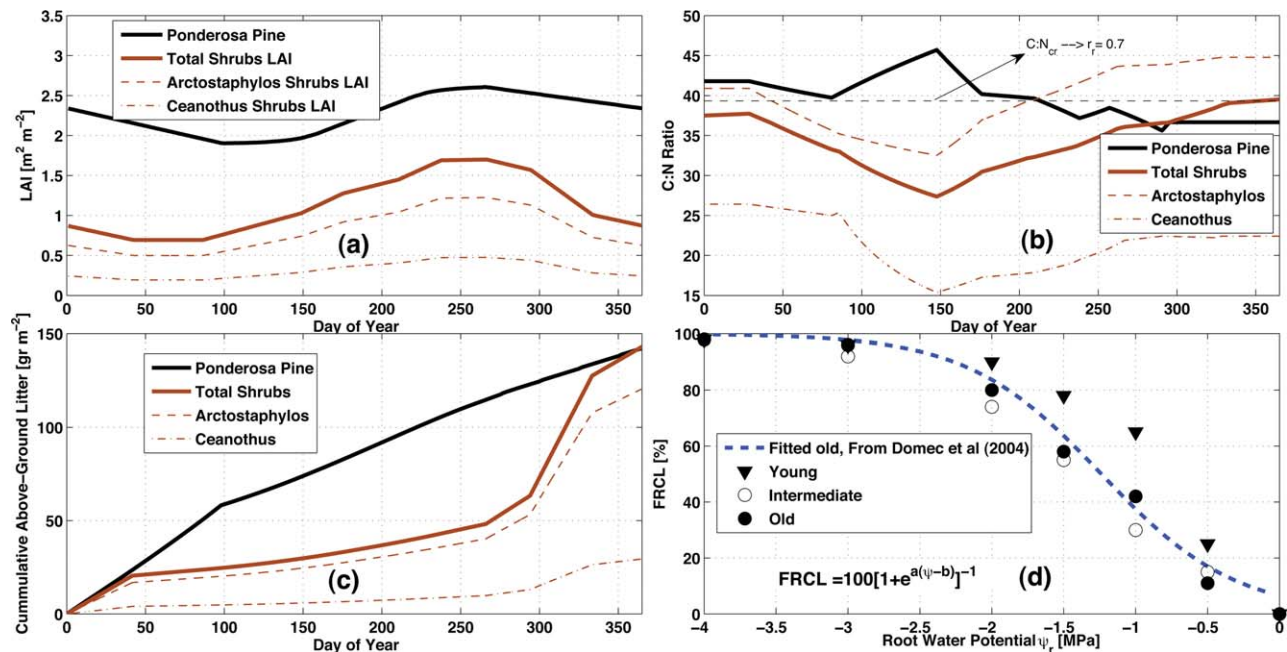


**Figure 3.** Annual time series of biogeochemical variables observed in Blodgett Forest such as (a) leaf area index (LAI), (b) C:N foliar ratio, and (c) annual cumulative above-ground input of carbon to the soil (online supporting information, section 3). This information is used to forced the biogeochemical C:N model. In this study, we assume that the time series of LAI, plant C:N ratios, and carbon input in the soil is the same for all the simulated years. This figure shows the time series for *Arctostaphylos* and *Ceanothus* shrubs individually. However, the simulations are performed considering all the shrubs as a one group where *Arctostaphylos* and *Ceanothus* are integrated by using a representative set of parameters and a combined LAI. (d) The fine root conductivity loss (FRCL) function for different ages of PP trees according to Domec *et al.* [2004]. In this study, we use the fitted line for old trees that is displayed. FRCL of 100% corresponds to no loss in conductivity.

based on available data from other locations [Jobbágy and Jackson, 2000; Fierer *et al.*, 2003]. Due to high uncertainty in the available records of  $\text{NO}_3^-$  and  $\text{NH}_4^+$  at Blodgett, we decided to set the initial concentrations in these pools to zero and perform the analysis once these pools reach equilibrium.

### 3. Results

#### 3.1. Moisture and Temperature Dynamics in the Soil Column

[25] Moisture and temperature play a crucial role in the carbon and nitrogen dynamics. Long and pronounced dry periods, such as those observed in Blodgett during summer, enhance the occurrence of strong gradients in water potential between the dry surface and deeper wet layers. The presence of a litter layer above the soil and the response of fine roots to dry conditions such as FRCL are mechanisms that may prevent the loss of moisture from the roots to the soil destined to feed soil evaporation under extreme dry conditions [Espeleta *et al.*, 2004]. A litter layer helps reduce, considerably, the efflux of water from the root to the soil under such situations and prevents root-soil hydraulic disconnection [Quijano *et al.*, 2012]. However, even in the presence of litter there is a flux of moisture from the roots that enhances soil evaporation [Quijano *et al.*, 2012].

[26] In the simulations performed under the No-HR case (scenarios II and IV), we imposed a complete hydraulic dis-

connection between the soil and the roots by setting the radial conductivity of the root system to zero (FRCL=1) whenever  $\psi_{\text{root}} > \psi_{\text{soil}}$ . This condition satisfies the no-water flux from the roots to the soil following the definition of No-HR and has been implemented in previous studies to perform the No-HR simulations [Amenu and Kumar, 2008; Quijano *et al.*, 2012].

[27] Figure 5 shows the FRCL for the topmost mineral soil layer located in horizon A1 (below horizon O) for the simulations performed with HR. Figure 5 shows the ensemble of FRCL for all the 500 years of simulation with dark line corresponding to year 100, which has been selected arbitrarily for illustration. Figures 5a and 5b show the FRCL function for the simulation with shrubs and No-shrubs, respectively. When HR is present (Figure 5), fine roots undergo a strong reduction in conductivity only during the summer period. The ensemble also shows that there is a considerable year to year variability as a result of variation in atmospheric forcing. In the No-HR simulation (not shown), there is a total hydraulic conductivity loss (FRCL=1) during the summer period that manifests after rainfall ceases at the beginning of the summer.

[28] As observed in Figure 5, in the presence of HR, FRCL never reaches 1. Although the uptake (or release) of moisture is reduced considerably, there is a continuous flux of moisture between the soil and roots. Furthermore, it can be observed that FRCL is consistently higher in the

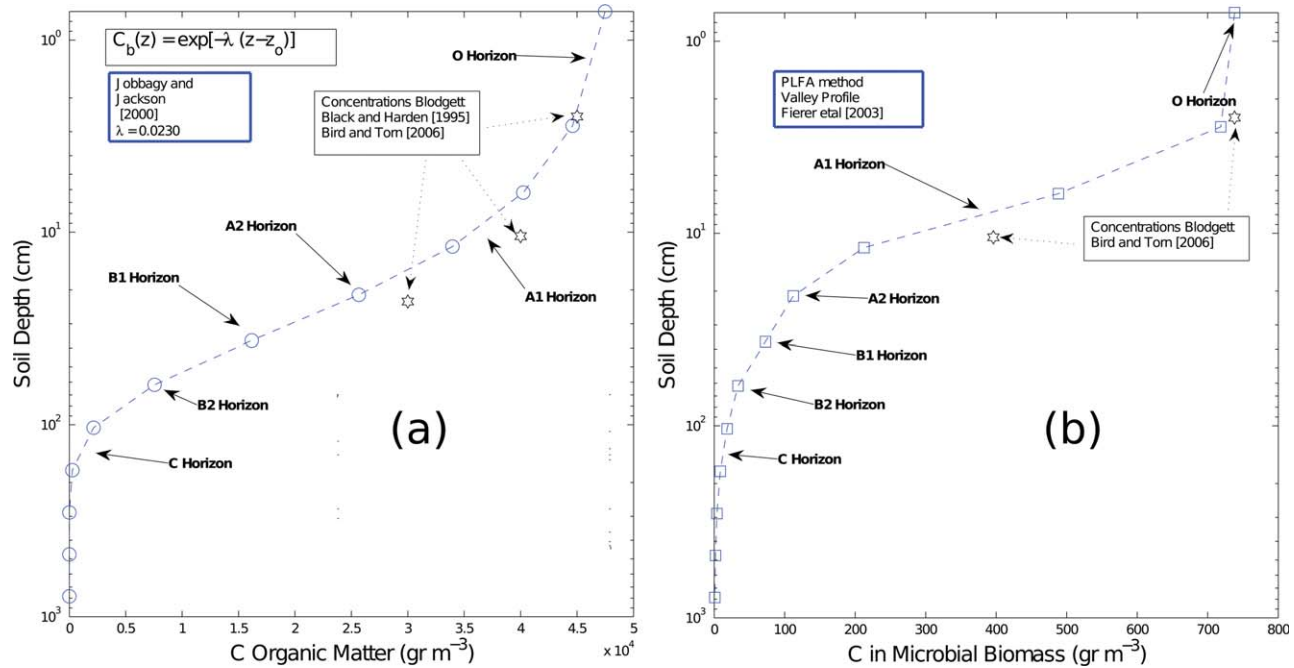


**Figure 4.** Initial conditions in the vertical distribution of soil carbon in the (a) organic matter  $C_s$  and (b) microbial biomass  $C_b$ . These profiles were derived from a combination of data collected at the Blodgett Forest (stars) and detailed profiles of  $C_s$  and  $C_b$  from other sites [Jobbágy and Jackson, 2000; Fierer et al., 2003].

presence of shrubs. This is because the presence of shrubs induces a more aggressive water uptake in the shallow soils that accelerates the reduction of soil moisture at the surface and, therefore, it impacts the fine root water potential.

[29] Understanding the fine root dynamics at the top of horizon A described above helps us examine in more detail the energy balance in the soil profile. Figure 6 shows the fluxes of moisture and states of temperature and moisture in the shallow soil (horizon O, A1, and A2) during the summer period.

[30] The absence of fine roots in the organic horizon results in no water uptake or release in this horizon. There is a prominent release of water from the roots to the soil in the top 2–5 cm of horizon A1. The release of moisture in this thin layer is higher than the release that takes place in the 5–10 cm domain. This pattern is observed both in the presence and absence of shrubs and is induced by the higher water potential gradients that occur between the root and the soil, which tend to increase toward the surface due to the evaporative demand. The efflux of water enhances the availability of moisture in these layers and supports soil evaporation. Figure 6b shows higher levels of soil moisture in the HR case for all depths displayed. Increases in soil evaporation during the summer reduce ground heat flux and surface and subsurface temperature. Therefore, the immediate result of No-HR is an increase in the soil temperature (see Figure 6c), where mean soil temperature in the No-HR case is consistently higher. Therefore, the net effect from the HR is a cooling effect with a reduction in soil ground heat flux.

[31] When shrubs are absent (Figures 6d–6f), lower LAI values allow higher radiative energy to reach the soil.

Although the amount of water released in the 2–5 cm of soil is similar in the absence and presence of shrubs, the net root uptake of moisture is higher when shrubs are present. In the presence of shrubs, there is a higher plant water demand and fine root biomass that compete with soil evaporation for available water in the soil. Therefore, in the absence of shrubs, HR enhances more soil evaporation compared with the case when shrubs are not present. As a result, the cooling effect caused by HR is more prominent in the absence of shrubs.

[32] The magnitude of the net release and uptake fluxes of moisture from plant roots at deeper layers (5–30 cm) are consistently higher in the presence of shrubs, which is expected due to gradients created from the large demand of water by the shallow rooted plants [Quijano et al., 2012].

[33] These differences in moisture and temperature stated between HR and No-HR and the presence and absence of shrubs affect the carbon and nitrogen dynamics as discussed below.

### 3.2. Steady-State Analysis of Carbon Dynamics

[34] The net impact of HR on organic matter decomposition can be explained as an interaction between soil moisture and soil temperature. This is conceptualized in the form of a simple product between  $f_D(\psi)$  and  $f_D(T)$ , which are the net effects of soil water potential and soil temperature on organic matter decomposition, respectively (online supporting information, equation (5)). Similarly, the net effect of HR in organic matter decomposition is represented by two main mechanisms: (i) redistribution of water in the soil column that enhances soil moisture in horizon A1 during the summer period and therefore enhances the



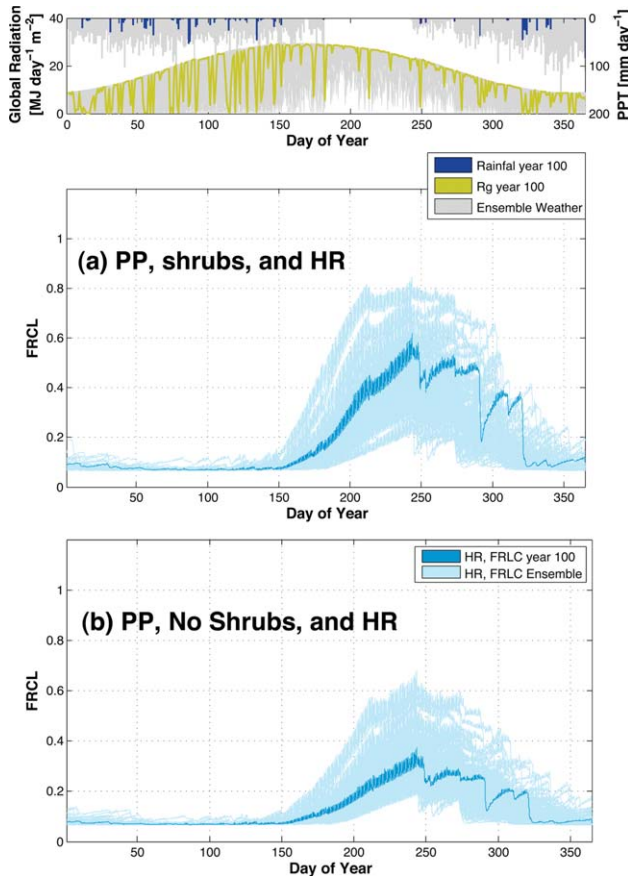


**Figure 5.** FRCL at the top 3 cm of horizon A1. FRCL represents the fraction of conductivity loss in fine roots as a response to dry conditions. The figures show the ensemble of FRCL for all the 500 years of simulation for the case when (a) shrubs are present and HR is active, and (b) shrubs are not present and HR is active. The darker lines show the FRCL for the simulations in year 100. This year was chosen arbitrarily to illustrate the dynamics in a particular year. (top) The realizations of rainfall and global radiation in blue and yellow, respectively, for year 100 and the ensemble of rainfall and radiation for 500 years in gray.

organic matter decomposition in horizons O and A1, where concentrations of organic carbon are the highest, and (ii) HR diminishes the ground heat flux and therefore reduces the temperature in the soil column (a cooling effect) resulting in a net decrement of organic matter decomposition.

[35] Figures 7a and 7b show the long-term annual decomposition rates of organic carbon (DEC) from the total soil column. The inset plots in Figures 7a and 7b show in more detail the first 30 years of simulation. During this transient period, both HR (blue) and No-HR (red) simulations diverge from the same initial conditions. For example, in the presence of shrubs it can be observed (inset in Figure 7a) that from year 1 to year 17 the decomposition rates are higher when HR is active. The enhancement in soil moisture at the top of horizon A1 overcomes the cooling effect when HR is active, resulting in higher decomposition rates. However, different decomposition rates impact the mass balance of carbon differently and after 17 years, the soil organic carbon pools ( $C_s$ ) diverge from the same initial con-

dition and become different ( $C_{s,HR} < C_{s,No-HR}$ ). Higher carbon content when HR is not active enhances decomposition in the following years. Thus, decomposition rates during years 18–23 become higher when HR is not active (inset in Figure 7a). In the long term, decomposition rates when HR is active (blue curves in Figures 7a and 7b) or not (red curves in Figures 7a and 7b) fluctuate around the same mean.

[36] Figures 7c and 7d show the dynamics of total  $C_s$  in the entire soil column. In the presence of shrubs (Figure 7c) the total  $C_s$  diverges from an initial condition of  $22 \text{ kg/m}^2$ . In the long term, it oscillates around a mean value close to  $26.8 \text{ kg/m}^2$ . The same dynamics are observed in the phase-space plot displayed in Figure 7e. On the other hand, Figures 7b, 7d, and 7f show the same information, but in this case the simulations are performed in the absence of shrubs. As expected,  $C_s$  converges to a lower value in the absence of shrubs fluctuating around a mean close to  $23.2 \text{ kg/m}^2$ .

[37] The dashed lines in Figures 7c and 7d represent the percentage difference in  $C_s$  between HR and No-HR, calculated as  $\Delta C_s = [(C_{s,HR} - C_{s,No-HR}) / C_{s,HR}] \times 100\%$ . In the presence of shrubs (Figure 7c), this difference oscillates below zero with a mean value of  $\overline{\Delta C_s} = -1.1\%$ , which suggests that there is a slightly higher accumulation of carbon in the absence of HR. Therefore, HR has a slightly net positive effect on decomposition that results in lower carbon content. Although the difference is small, it suggests that the net enhancement of soil moisture in horizon A1 during the summer period overcomes the cooling effect when HR is active.

[38] In the absence of shrubs, there is a positive accumulation of carbon when HR is active (Figure 7d) with a mean  $\overline{\Delta C_s} = +1.9\%$ . In this case, the decomposition is higher when HR is not active, which suggests that the cooling effect is overcoming the enhancement due to moisture in horizon A1. As shown in section 3.1, the differences in soil evaporation and soil temperature when the simulations are performed with or without HR are more prominent in the absence of shrubs. These results suggest that the impact of the cooling effect translated as the difference in decomposition of organic matter between the simulations performed with HR and without HR is more prominent in the absence of shrubs. Lower LAI and lower plant transpirational demand in the absence of shrubs results in a higher soil evaporation water demand that enhances the cooling effect from HR. Therefore, in very dense canopies, the impact of the cooling effect from HR may become insignificant even during periods of high global radiation. If the cooling effect becomes insignificant, the only effect of HR on decomposition of organic carbon is only moisture dependent.

[39] The presence of HR also influences the distribution of  $C_s$  in the soil column. HL efflux to horizon A1 during the summer period and HD efflux to horizon C1 during winter periods enhance decomposition in these horizons. Deeper layers ( $>2.3 \text{ m}$ ) see a lower mean annual soil moisture in the presence of HR as a result of decreased drainage [Amenu and Kumar, 2008] (this is discussed further in section 3.3). The inset plots in gray colors in Figures 7e and 7f show the mean differences in  $C_s$  for each horizon. The presence of HR results in lower  $C_s$  in horizons O, A1, and C. There is a higher accumulation of  $C_s$  at depth greater



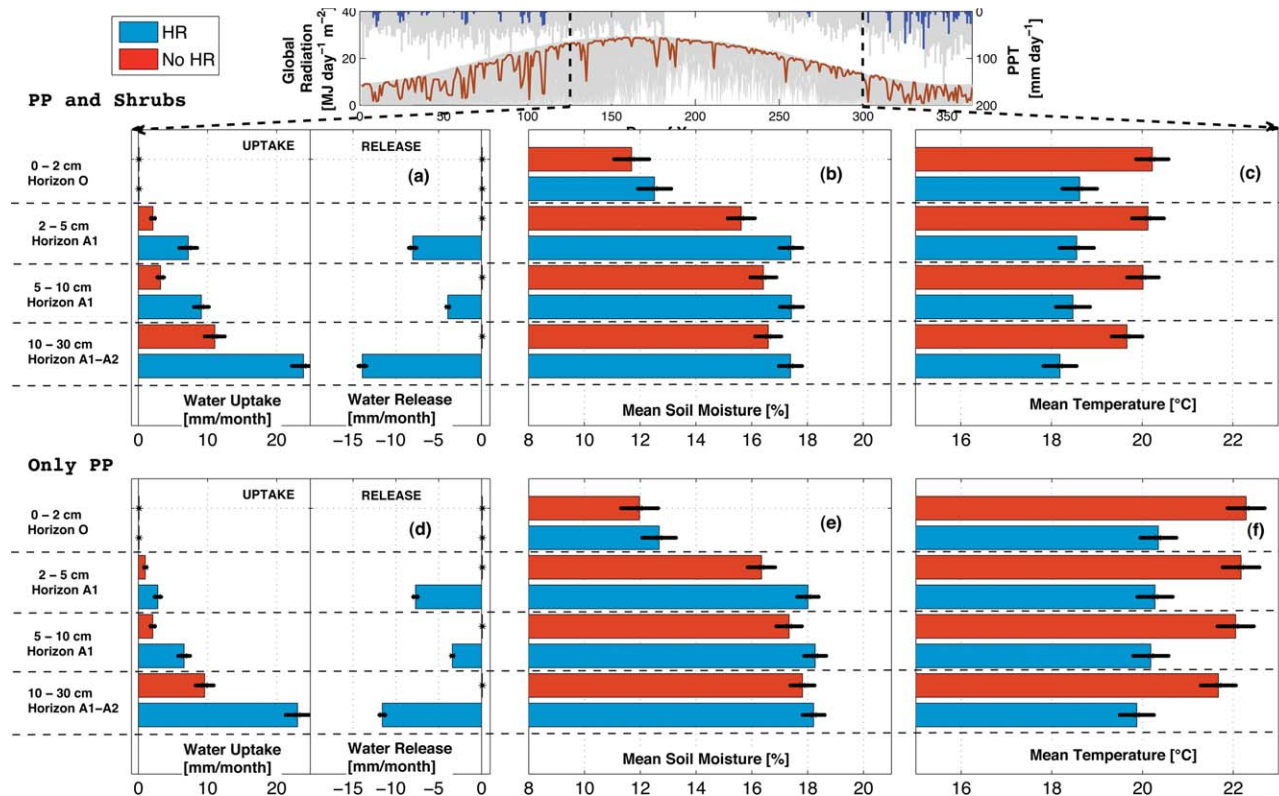


**Figure 6.** Energy balance at the surface and implications on (a and d) water fluxes, (b and e) soil moisture states, and (c and f) soil temperature in the shallow layers during the summer period. The simulations in the (top) presence of shrubs and (bottom) absence of shrubs. The small figure at the top displays the ensemble of 500 years of precipitation and global radiation. The bar sizes represent the mean values involved during 250–500 years of simulation and the standard deviation is represented by the black line.

than 2.3 m. In deep horizons, the input of organic matter as well as the rates of decomposition and mineralization are much lower compared to the surface. In the long term, these horizons may play a role, particularly when we compare the simulations between HR and No-HR (Figures 7e and 7f).

[40] The inset plots in blue (HR) and red (No-HR) in Figures 7e and 7f show the difference in  $C_s$  in the presence and absence of shrubs ( $C_{s,shrubs} - C_{s,No\ shrubs}$ ). The most prominent difference occurs in horizon A1. Also note that the differences are notably higher in the No-HR case. The net difference in soil temperature between the simulations performed with and without HR is stronger when shrubs are absent, because the impact of the cooling effect is more prominent. Higher differences in soil temperature also result in higher differences in decomposition between HR and No-HR cases.

[41] The magnitude of the cooling effect produced by HR is regulated by the presence and functioning of fine roots at the surface. The results displayed in Figure 7 were simulated using the soil structure described in section 2, with no fine roots in the litter layer and no fine roots in horizon O. Figure 8 shows a sensitivity analysis comparing the simulations for different locations of fine roots. The simulations in green color were performed by assuming the presence of fine roots in the organic horizon, while the simulations in yellow assume that there are no fine roots either

in the organic horizon or in the top 3 cm of horizon A1. When shrubs are present (Figure 8a), fine roots located in the organic horizon enhance the cooling effect when HR is active. Therefore, it produces a negative effect on decomposition throughout the soil column, resulting in a considerable accumulation of  $C_s$  with a mean annual  $\Delta C_s = +8.2\%$ . The absence of fine roots in the top 3 cm of horizon A1 considerably reduces the cooling effect, and the net impact of HR on decomposition is only due to redistribution of moisture in the soil column. The reduction of the cooling effect creates a net positive effect on decomposition when HR is active, and this results in a lower  $C_s$  in the long term, with a mean annual  $\Delta C_s = -3.5\%$ .

[42] Figure 8b displays the sensitivity analysis in the absence of shrubs. As mentioned before, in the absence of shrubs the impact of the cooling effect by HR is more prominent, and consequently the difference in carbon content with and without HR ( $\Delta C_s$ ) is higher in the absence of shrubs. The sensitivity analysis in the absence of shrubs shows that for the case when fine roots are located in the horizon O there is a mean annual  $\Delta C_s = +9.7\%$ . On the other hand, the absence of fine roots at the top of horizon A1 results in a mean annual  $\Delta C_s = -2.5\%$ .

[43] Figure 8 (bottom) shows mean percentage difference in  $C_s$ , for each horizon in the soil. The results displayed in these panels suggest that the cooling effect regulated by the presence or absence of fine roots in

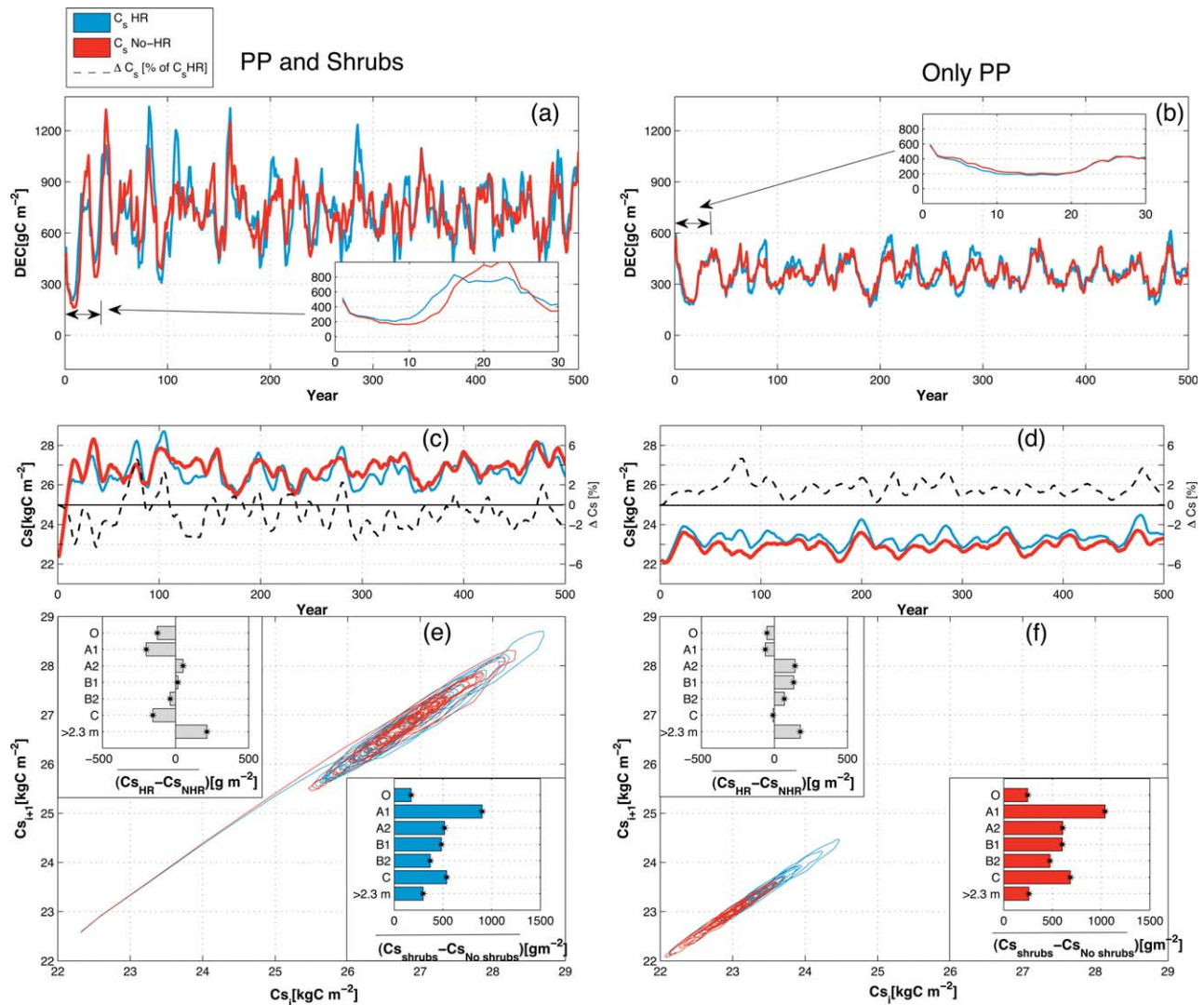


**Figure 7.** Long-term dynamics of carbon in the soil organic matter. (a and b) The long-term simulation results of soil decomposition in  $\text{g C m}^{-2}$ . (c and d) The long-term simulation results of carbon in the soil organic matter  $C_s$  in  $\text{kg C m}^{-2}$ . (e and f) The phase space of carbon in the organic matter ( $C_{s,i+1}$ ,  $C_{s,i}$ ) in  $\text{kg C m}^{-2}$ . The inset figures in gray color on the Figures 7e and 7f show the mean carbon differences in  $C_s$  between HR and No-HR at each horizon. Similarly the inset figures in blue and red color on the Figures 7e and 7f show the mean carbon differences in  $C_s$  between the simulations when shrubs are present or absent. The blue and red colors in the figure reflect the simulations in the presence or absence of HR respectively.

horizon O and horizon A1 impact the long-term accumulation of carbon in the entire soil column. The results in Figure 8 suggest that fine roots and their interplay with HR have important implications on the soil carbon cycle not only by their biomass contribution [Jackson *et al.*, 1997; Richter *et al.*, 1999] but also by their control on the energy and moisture dynamics at the surface. Figures 9a and 9c show the annual cycle for soil temperature at 5 cm and heterotrophic respiration from the entire soil column (Figures 9b and 9d). Numerical simulations of temperature show a good agreement most of the year except in the late summer where the model overestimates. However, we note that the model temperature corresponds to average values over the canopy footprint while the observation was recorded from a single-point measurement during years 2000–2005.

[44] According to the results presented in this section, the net annual decomposition (also the heterotrophic respiration) at equilibrium is similar between the simulations performed with and without HR (Figures 7a and 7b). However, at equilibrium, the content of carbon in the soil varies between the simulations performed with and without HR (Figures 7 and 8), and these dynamics depend on the presence and absence of shrubs and are highly sensitive to the location and functioning of fine roots in the surface. The interannual patterns of decomposition (also heterotrophic respiration) at equilibrium are consistently different when the simulations are performed with and without HR. Figure 9 shows the interannual fluxes of heterotrophic respiration for the scenarios when shrubs are present (Figure 9b) and absent (Figure 9d). During the dry summer period, the

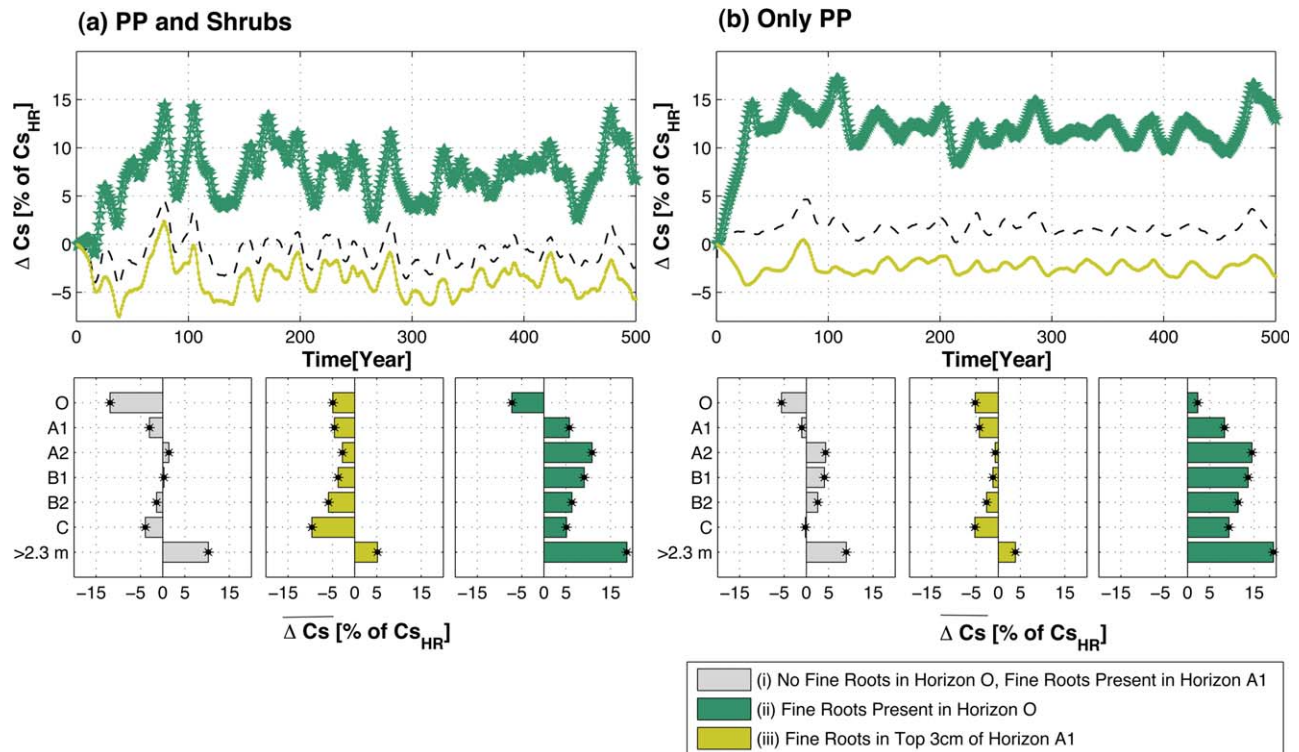


**Figure 8.** Sensitivity analysis on fine-root functioning and presence at the top surface. Three different simulations are compared (i) In gray color: no fine roots in horizon O and fine roots present in horizon A1 (as observed in available information documented at Blodgett Forest), (ii) In green color: fine roots present in horizon O and fine roots present in horizon A1, (iii) In yellow color: no fine roots present in horizon O and no fine roots present in top 3 cm of horizon A1. (top) The results for the long-term percentage difference in carbon accumulation between the presence and absence of HR. This difference is defined as  $\Delta C = \frac{C_{s,HR} - C_{s,No-HR}}{C_{s,HR}}$ . (bottom) The mean carbon percentage difference  $\overline{\Delta C_s}$  for each horizon for each of the three simulations considered.

heterotrophic respiration is higher when HR is active (blue curves in Figures 9b and 9d). However, heterotrophic respiration is higher in the rest of the year for the simulations without HR (red curves). These differences are more prominent in the presence of shrubs (Figure 9b) because there is a higher amount of fine roots in shallow layers that enhances the redistribution of moisture to horizon A1, and the impact of the cooling effect is less strong in the presence of shrubs. These processes allow the simulations with HR to have a considerable higher heterotrophic respiration (decomposition) during the summer dry period compared with the simulations performed without HR.

### 3.3. Steady-State Analysis of Nitrogen Dynamics

[45] The dynamics of nitrogen in the subsurface includes mineralization, immobilization, nitrification, and leaching, and is tightly coupled to subsurface carbon cycling [Porporato *et al.*, 2003; D'Odorico *et al.*, 2003; Manzoni and Porporato, 2007]. In this section, we examine how HR and the presence or absence of shrubs impact the fluxes of mineral nitrogen ( $\text{NH}_4^+$ ,  $\text{NO}_3^-$ ).

[46] The uptake by plant roots is the most important flux that depletes the mineral nitrogen from the soil and, therefore, it plays an important role in the mass balance of nitrogen in the soil. In this study, the uptake of mineral nitrogen

by plant roots is simulated by the consideration of two main mechanisms of nitrogen uptake: (i) uptake of mineral ions that are brought toward the roots with the water flux (passive uptake) and (ii) uptake of mineral ions that are brought toward the roots by a diffusion pathway in the soil (active or diffuse uptake) [Porporato *et al.*, 2003]. The passive uptake flux is computed as the advective flux of mineral nitrogen that is transported by the transpirational current. On the other hand the active uptake is computed according to the capacity of roots per unit of dry biomass to uptake mineral nitrogen from a diffusive pathway,  $F_{\text{factor}}$  (Table 1), which is based on the initial approach of Porporato *et al.* [2003] and modified here in the light of a multi-layer and multispecies framework. The equations used to simulate these processes are described in more detail in the online supporting information (section 2).

[47] Figure 10 shows the mean annual water and  $\text{NO}_3^-$  fluxes, and  $\text{NO}_3^-$  concentration in different horizons. The uptake of water is enhanced in the presence of HR (blue lines in Figure 10). Similarly, the presence of shrubs enhances the uptake of water because they increase the transpirational demand. As a result the lowest mean water drainage from all the different scenarios considered occurs in the presence of shrubs and when HR is active. The fluxes of mineral nitrogen, particularly  $\text{NO}_3^-$ , are coupled with those



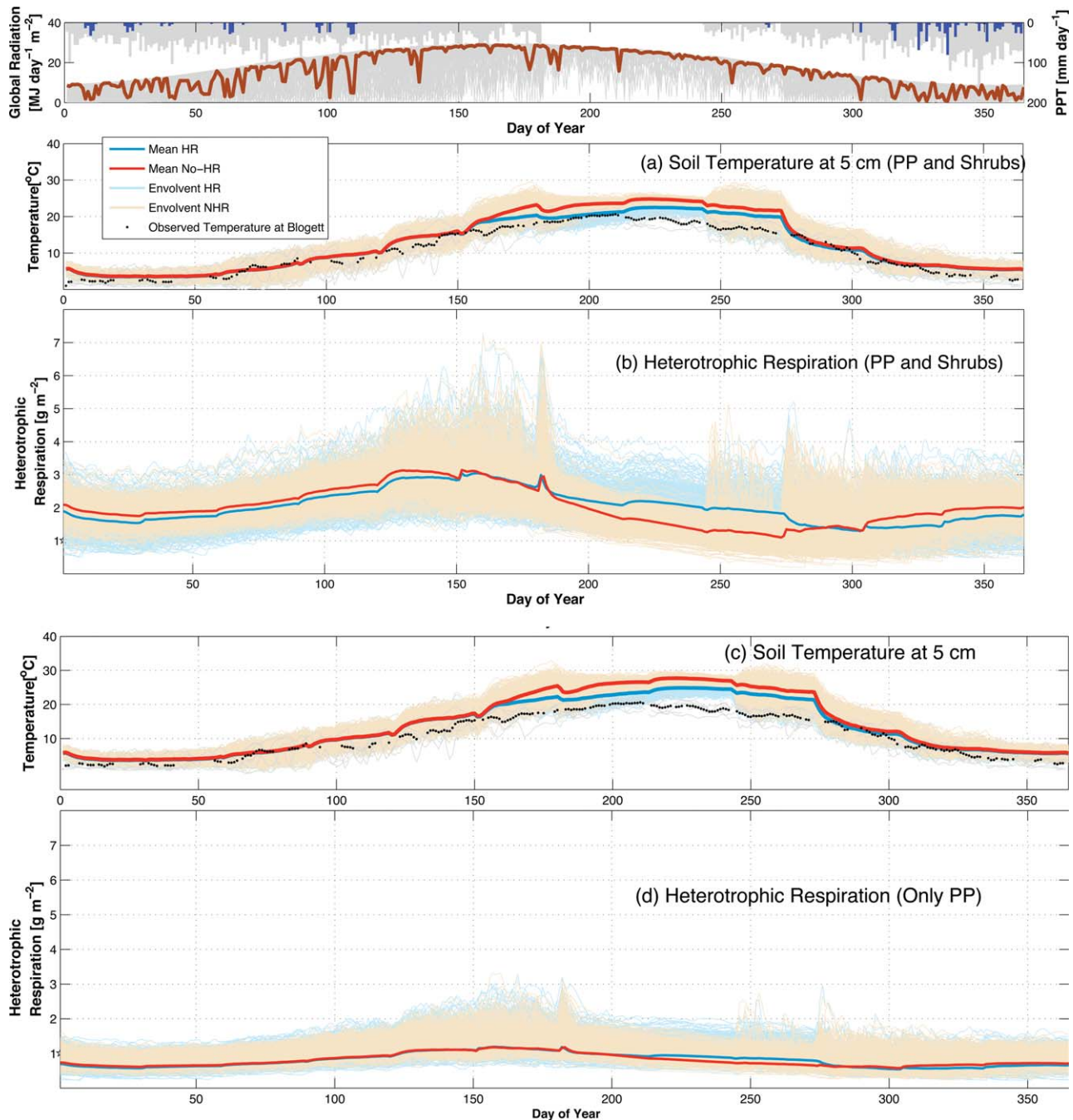


**Figure 9.** The simulation of (a and c) soil temperature at 5 cm and (b and d) soil respiration. (top) The simulations of precipitation and global radiation. The pattern of global radiation is observed in the temperature and heterotrophic respiration plots. Lighter lines in Figures 9a–9d show the ensemble of simulations results during 250–500 years. On the other hand, the thicker lines represent the average over all these years of simulation.

of moisture. However, the highest uptake of  $\text{NO}_3^-$  occurs in horizon A1 while the highest uptake of water occurs from the deepest layers. During the dry summer period, this ecosystem sustains a high transpiration rate that relies on deep root water uptake [Quijano *et al.*, 2012]. However, plant roots are able to uptake  $\text{NO}_3^-$  from the soil by a diffusive pathway (active) even during periods of low soil moisture and no water uptake. The highest allocation of roots

occurs in shallow horizons, and therefore the highest uptake of  $\text{NO}_3^-$  takes place from these horizons by an active uptake. These results show the relevance of the active uptake of  $\text{NO}_3^-$  in ecosystems experiencing long and prolonged dry periods such as Blodgett.

[48] Although the active mechanism plays a critical role in the net uptake of mineral nitrogen, the passive mechanism is also important. The  $\text{NO}_3^-$  concentration in the soil

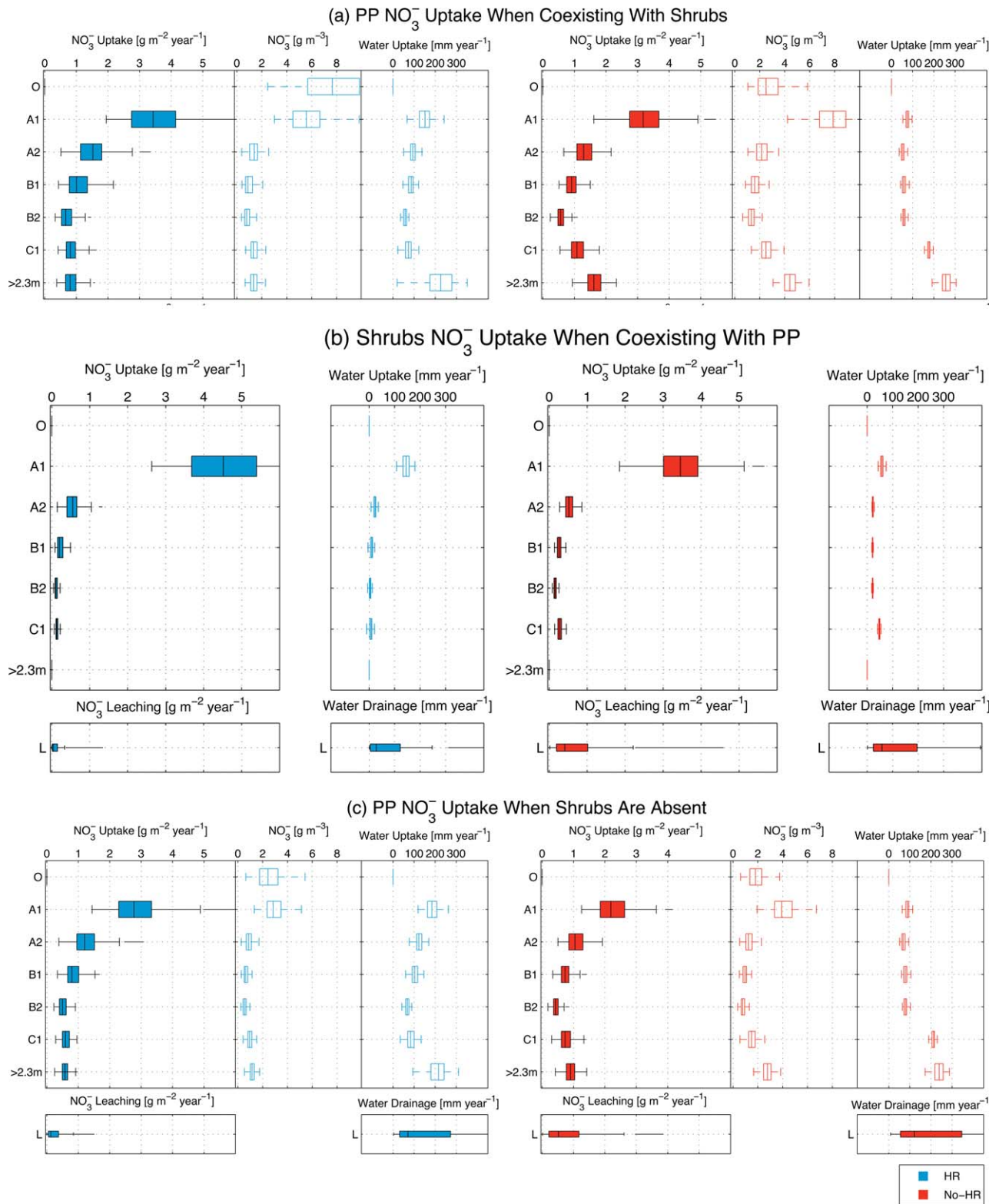


**Figure 10.** Dynamics of water and  $\text{NO}_3^-$  uptake in the presence and absence of shrubs. The variables displayed are mean annual  $\text{NO}_3^-$  uptake, mean annual  $\text{NO}_3^-$  concentration, and mean annual water uptake. The box plots show the summary for all the simulations performed between 250 and 500 years which is considered a period where steady solutions have been already reached. (a and b) The simulation results for the case when both species, PP and shrubs, coexist. Figure 10a shows the uptake of  $\text{NO}_3^-$  and water by only PP, and Figure 10b shows the uptake of  $\text{NO}_3^-$  and water only by shrubs. (c) The simulation results in the absence of shrubs (PP being the only species). HR enhances plant uptake of  $\text{NO}_3^-$  from shallow layers and reduces leaching. In the absence of HR, the concentrations of  $\text{NO}_3^-$  are higher in deeper layers. The presence of understory shrubs with smaller foliar C:N ratios increases the pool of nitrogen in the soil enhancing PP  $\text{NO}_3^-$  uptake.

**Table 2.** Total Annual Nitrogen Fluxes<sup>a</sup>

Uptake Form	HR		No-HR	
	PP	Shrubs	PP	Shrubs
N uptake	8.77 (0.38)	5.46 (0.53)	8.98 (0.52)	4.58 (0.70)
NO <sub>3</sub> <sup>-</sup> uptake <sup>b</sup>	6.27 (0.37)	4.08 (0.52)	7.03 (0.48)	3.52 (0.70)
NH <sub>4</sub> <sup>+</sup> uptake	2.50 (0.42)	1.38 (0.53)	1.95 (0.62)	1.06 (0.69)
Total N uptake	14.24 (0.44)		13.47 (0.54)	
Leaching <sup>b</sup>	0.10		0.70	
Only PP				
N uptake	6.92 (0.32)		6.32 (0.46)	
NO <sub>3</sub> <sup>-</sup> uptake <sup>b</sup>	4.72 (0.30)		4.73 (0.43)	
NH <sub>4</sub> <sup>+</sup> uptake	2.19 (0.37)		1.59 (0.54)	
Total N uptake	6.92 (0.32)		6.32 (0.46)	
Leaching <sup>b</sup>	0.24		0.83	

<sup>a</sup>The fluxes displayed correspond to multiannual average computed with the simulations results obtained between years 250 and 500. All the fluxes are in gm<sup>-2</sup>year<sup>-1</sup>. Values in parenthesis represent  $f_{\text{diff}}$ : the fraction of the flux that arrives by a diffusion pathway.

<sup>b</sup>Same as displayed in Figure 10.

column (Figure 10) is highest at the top in horizon A1. This is expected since mineralization occurs mostly in horizon A1, and the input of mineral nitrogen from atmospheric deposition is allocated to horizon O. However, there are some differences in the distribution of the NO<sub>3</sub><sup>-</sup> concentration between the simulations performed with (blue boxes) and without (red boxes) HR. When HR is active, the distribution of NO<sub>3</sub><sup>-</sup> follows an exponential decay with a maximum value at the top that decreases with depth. On the other hand, when HR is not active, the vertical distribution of NO<sub>3</sub><sup>-</sup> presents a C shape that is maximum at the top, but it also increases at the bottom. The high uptake of water from shallow layers when HR is active reduces the drainage of moisture in the soil column and enhances the passive uptake of NO<sub>3</sub><sup>-</sup> from these layers. When HR is not active, there is a higher leaching of NO<sub>3</sub><sup>-</sup> and therefore a higher accumulation in deeper horizons.

[49] Note also that the vertical distribution of NO<sub>3</sub><sup>-</sup> in the soil column influences the dynamics of NO<sub>3</sub><sup>-</sup> uptake since the uptake from both mechanisms (passive and active) is concentration dependent. This is observed in the vertical distribution of NO<sub>3</sub><sup>-</sup> uptake (Figure 10) that follows a similar shape as the distribution of NO<sub>3</sub><sup>-</sup>. However, the uptake of NO<sub>3</sub><sup>-</sup> in the top horizons is more accentuated, since in these horizons there is greater root biomass.

[50] The presence of shrubs increases the pool of nitrogen in the soil due to lower C:N ratios in the foliage in comparison to PP. As a result, in the presence of shrubs, the concentration and uptake of NO<sub>3</sub><sup>-</sup> are higher. Although the presence of shrubs increases the pool of nitrogen in the soil, it does not increase the net leaching of NO<sub>3</sub><sup>-</sup> out of the root zone. In the case of HR, the introduction of shrubs results in lower leaching of NO<sub>3</sub><sup>-</sup> out of the root zone. This arises because shrubs uptake NO<sub>3</sub><sup>-</sup> and also because the enhanced transpiration reduces the net drainage of water from the root zone (Figure 10).

[51] Table 2 summarizes the net magnitude for each of the uptake and leaching fluxes described above. It also shows in parenthesis the respective values of the diffuse uptake fraction ( $f_{\text{diff}}$ ), which is defined as the ratio between the uptake flux that originates from a diffusive pathway and the total uptake flux (online supporting information, equa-

tion (20)). The parameter  $f_{\text{diff}}$  ranges between 0.3 and 0.7. This fraction varies according to the type of flux and also with the presence of HR. As expected, the fraction from a diffuse pathway is higher for NH<sub>4</sub><sup>+</sup> compared to NO<sub>3</sub><sup>-</sup> uptake. Also, when HR is active, the percentage of mineral nitrogen uptake fluxes from a diffuse pathway is lower compared to the simulations when HR is not active. These results suggest plants may rely more on a diffuse pathway when HR is not active.

[52] When shrubs and PP coexist, there is a higher uptake of mineral nitrogen from PP compared to the scenario when shrubs are absent. The leaching of NO<sub>3</sub><sup>-</sup> lost out of the root zone is around 0.6 g/yr lower when HR is active. This difference may become an important amount in the long term, particularly in the absence of shrubs, where the only external input of nitrogen is from atmospheric deposition.

[53] Figure 11 shows the long-term dynamics of mineral nitrogen content in the entire soil column. Figures 11a and 11b display NO<sub>3</sub><sup>-</sup> and Figures 11c and 11d display NH<sub>4</sub><sup>+</sup> dynamics. The patterns observed are similar to those observed in carbon dynamics. The initial conditions are established as no mineral nitrogen content in the soil column. After about 250 years, the content of NH<sub>4</sub><sup>+</sup> and NO<sub>3</sub><sup>-</sup> reaches equilibrium with oscillations around a mean value. As observed in all of the plots in Figure 11, the absence of HR results in a higher content of mineral nitrogen in the soil. Shrubs increase the input pool of nitrogen in the soil. However, there is no significant difference in mineral nitrogen content between the presence or absence of shrubs when HR is active (compare blue lines in Figures 11a and 11b), which suggest that plants are able to enhance their uptake under higher nitrogen when shrubs are present. On the other hand in the No-HR case, higher increments in the nitrogen pool that occurs in the presence of shrubs results in higher mineral nitrogen content in the soil (Figure 10).

[54] According to the results in Figures 10 and 11 and Table 2, the presence of both shrubs and HR reduces the leaching of nitrogen from the soil column. However, these results may be sensitive to other external processes:

[55] (i) The rate of transformation from NO<sub>3</sub><sup>-</sup> to NH<sub>4</sub><sup>+</sup> (nitrification rate): If there is less NO<sub>3</sub><sup>-</sup> production, the retention time of mineral nitrogen in the root zone will increase and therefore the rate of leaching will be lower. This process is regulated by the nitrification factor  $k_n$  (see online supporting information, section 2, equation (14)).

[56] (ii) The ability of roots to uptake nitrogen by a diffusive pathway: If roots increase their capacity to uptake water by diffusion, they will become less vulnerable to loss of mineral nitrogen by leaching. This process is regulated by parameter  $F_{\text{factor}}$  (see online supporting information, section 2, equation (18)).

[57] All the simulation results displayed in this document were performed with the values of  $F_{\text{factor}}$  and  $k_n$  shown in Table 1. Figure 12 displays a sensitivity analysis showing the influence of  $k_n$  and  $F_{\text{factor}}$  on the net leaching of nitrogen out of the root zone. In Figure 12 the stars represent the simulation results when shrubs are present, while the circles represent the case at which shrubs are absent. Similarly the blue color represents the simulation results when HR is active and the red represents the simulation results when HR is not active. The size of the circles represents



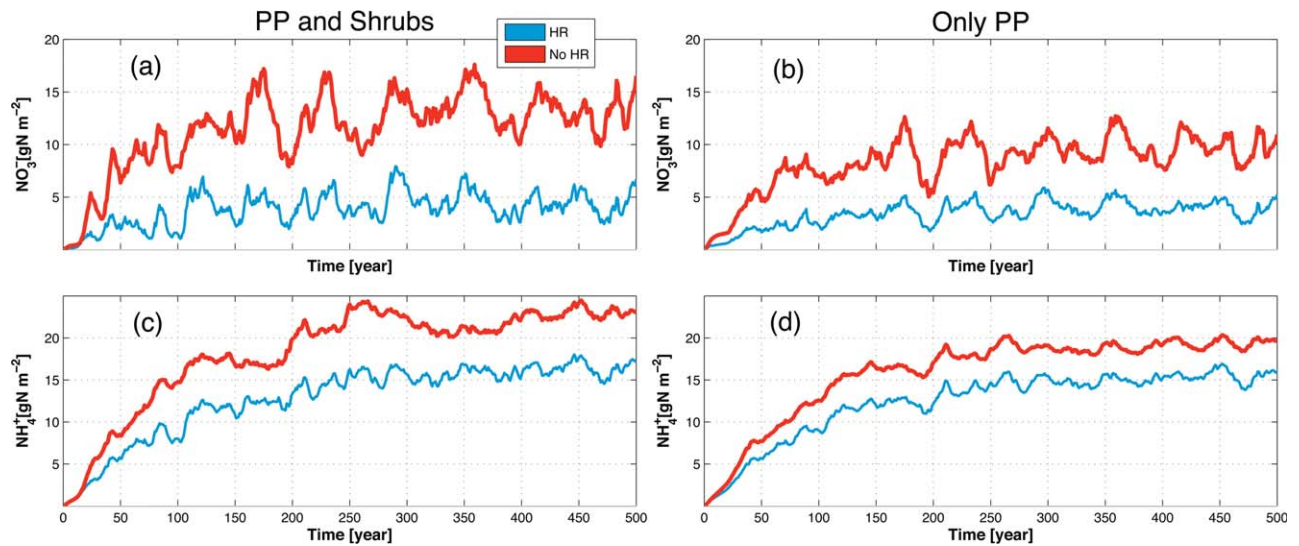


**Figure 11.** Long-term simulation results of (a and b) total  $\text{NO}_3^-$  content and (c and d) total  $\text{NH}_4^+$  content in the soil column.

the fraction from the total mineral nitrogen uptake that comes from a diffusive pathway ( $f_{\text{diff}}$ ). Each point in Figure 12 was generated with an independent simulation of 500 years with a unique combination of  $F_{\text{factor}}$  and  $k_n$ . The values displayed in this figure represent the mean annual average leaching of mineral nitrogen out of the root zone during years 250–500.

[58] As expected, higher  $F_{\text{factor}}$  and lower  $k_n$  results in lower leaching of  $\text{NO}_3^-$ . The movement of nitrogen ions in the soil can be conceived as a trade-off between *horizontal fluxes* such as the water uptake stream (forced by gradients in soil water potential) and diffusion (forced by gradients in soil ion concentration) that pulls ions toward the fine roots, and *vertical fluxes* such as drainage that are produced by

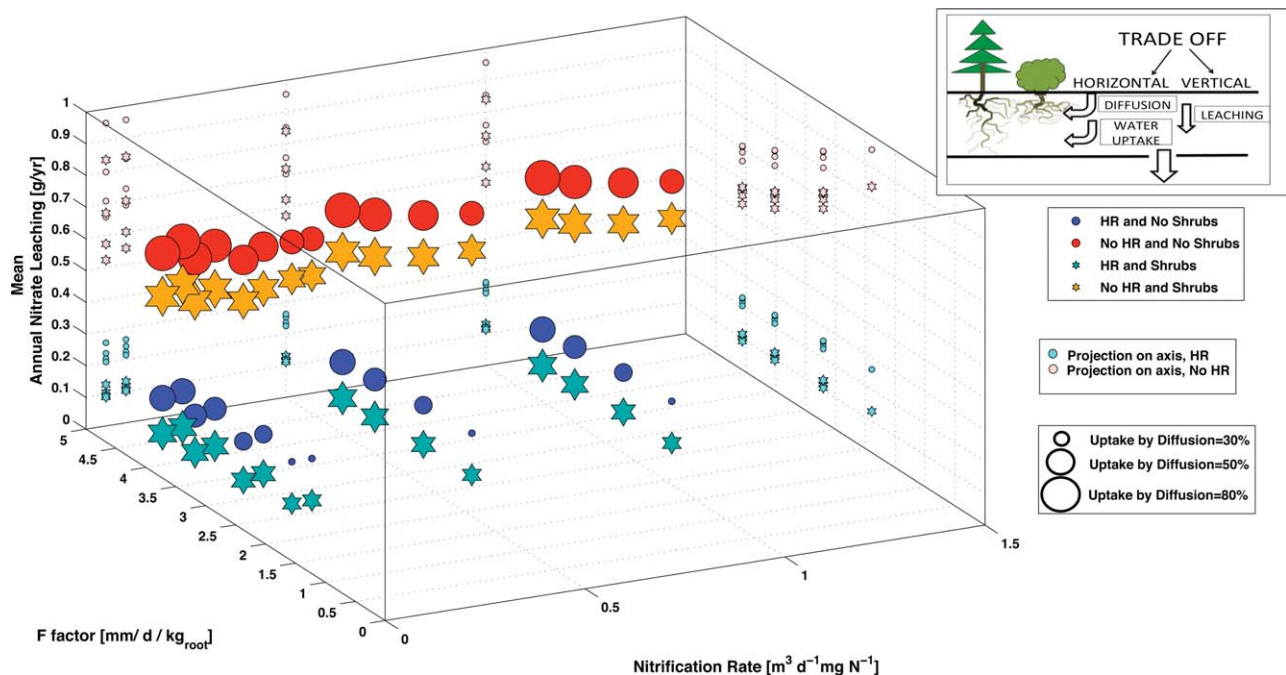


**Figure 12.** Trade-off between nitrification rate ( $k_n$ ), root diffusion nitrogen uptake factor ( $F_{\text{factor}}$ ), and total leaching of mineral nitrogen from the root zone. Higher rates of nitrification enhances  $\text{NO}_3^-$  leaching while higher  $F_{\text{factor}}$  reduces  $\text{NO}_3^-$  leaching. Both the presence of shrubs and the presence of HR reduce the leaching of  $\text{NO}_3^-$ . The size of the symbols represent the fraction of nitrogen uptake from a diffusive pathway ( $f_{\text{diff}}$ ). Under the same combination of  $k_n$  and  $F_{\text{diff}}$ , this fraction is lower when HR is active. These results suggest the net uptake of nitrogen rely more on a diffusively pathway when HR is absent and therefore this scenario is more sensitive to  $k_n$  and  $F_{\text{factor}}$ .

the effect of gravity. The trade-off is supported by the fact that stronger horizontal fluxes result in weaker vertical fluxes or vice versa. This effect can be seen in Figure 12 where the presence of HR and different plant species enhances horizontal fluxes (water uptake) and reduce the vertical flux represented by  $\text{NO}_3^-$  leaching. Moreover, higher diffusion capacities (higher  $F_{\text{factor}}$ ) also enhance horizontal fluxes causing a reduction in  $\text{NO}_3^-$  leaching.

[59] However, the effect of increasing the diffusion capacity is more sensitive when HR and shrubs are absent. If HR and shrubs are present, their ability to intensify the water uptake flux is able to capture the amount of nitrogen uptake that is missed by a reduction in diffusion if the diffusion pathway uptake capacity from the roots (which is conceptualized in terms of  $F_{\text{factor}}$ ) was reduced. In Figure 12, the magnitude of  $f_{\text{diff}}$  is represented by the size of the symbols. It can be observed that under low values of  $F_{\text{factor}}$ , the presence of shrubs and HR results in small sizes that indicates a low fraction from a diffusive pathway. Under the same values of  $F_{\text{factor}}$ , the  $\text{NO}_3^-$  leaching is considerably higher in the absence of both shrubs and HR. The simulations results presented in Figure 12 suggest that the presence of HR and different species enhances the ability of ecosystems to uptake ions such as  $\text{NO}_3^-$  and reduces the dependence of plant roots to uptake mineral nitrogen by diffusive pathways from the soil.

#### 4. Summary and Conclusions

[60] In this study, we analyze how the interplay between HR and multiple plant species affect the below-ground dynamics of carbon and nitrogen. The analysis enabled the assessment of the long-term impact of this interplay in the pools of carbon and nitrogen in the soil.

[61] Findings indicate that the presence of HR influence decomposition of organic matter by two mechanisms. First, it modifies soil moisture throughout the soil column and favors decomposition in horizons A1. Second, HR reduces the soil temperature (cooling effect), resulting in reduced decomposition rates throughout the soil column. Decomposition rates are also a function of the total soil carbon,  $C_s$ , and the microbial pool,  $C_b$ . After a transient response, there is convergence toward different states of  $C_s$  concentration but with nearly the same decomposition rates. Therefore, in the long term, HR impacts the size of  $C_s$  pools rather than the decomposition rates.

[62] The cooling effect observed in the presence of HR varies according to the amount of energy that reaches the soil. We found that it is more prominent when shrubs are absent. In the presence of shrubs, the reduction of radiation reaching the ground surface due to higher LAI reduces the soil evaporation. As a result, HR is less influential in affecting the soil evaporation and the ground heat flux. These dynamics suggest that in dense canopies the cooling effect may not be seen. In addition, the cooling effect is a function of the location of fine roots and their functioning. The presence of fine roots that release water through HR magnifies the cooling effect, resulting in higher accumulation of  $C_s$ . On the other hand, if fine roots are located deeper into the soil the cooling effect is less prominent.

[63] Presence of shrubs increases the flux of organic matter in the soil, resulting in higher concentrations of organic

carbon. The most prominent enhancement of  $C_s$  in the presence of shrubs is observed in the near-surface soil horizons. Furthermore, under the presence of shrubs heterotrophic respiration from the soil is considerably higher.

[64] The presence of shrubs also increases the input fluxes of nitrogen in the soil. Coexisting species such as PP are able to uptake more nitrogen from the soil, therefore they are favored by the presence of shrubs. The simulations show an interesting interplay between shrubs and HR. HR reduces the leaching of mineral nitrogen by enhancing the ability of plants to capture available nitrogen in shallow horizons with the transpirational stream through passive uptake. Shrubs also extend the ability of the system to capture nitrogen by allocating roots in shallow layers and also by increasing water uptake from the soil for transpiration which in turn reduces drainage. The lowest leaching of  $\text{NO}_3^-$  was attained when both shrubs and HR were present. These results suggest that HR and coexistence of different species reduce leaching of  $\text{NO}_3^-$  from the root zone. In addition, the net content and the distribution of mineral nitrogen along the soil profile are influenced by HR. Higher leaching of nitrogen to deeper layers results in more nitrogen allocated in deeper layers in the absence of HR. This phenomenon is more prominent when shrubs are present.

[65] In temperate natural ecosystems, nitrogen is often a limited nutrient. The results in this study show that under the presence of HR the ecosystem is more efficient in reducing the leaching of nitrogen from the root zone, resulting in a lower mean  $\text{NO}_3^-$  leaching flux of  $0.6 \text{ g/m}^2/\text{yr}$ . The capacity of the ecosystem to reduce  $\text{NO}_3^-$  leaching, even in low magnitudes could be an important trait.

[66] Further, the uptake of mineral nitrogen under the same conditions of fine root biomass, fine root distribution, and diffusion uptake factors ( $F_{\text{factor}}$ ) are higher when HR is active. Previous studies have mentioned two relevant processes that enhance the retention of nitrogen in the soil: (i) micro-organisms [Vitousek and Matson, 1984] and (ii) species diversity [Hobbie, 1992]. Our results provide support for the latter where the interplay between different species as a proxy of plant biodiversity, and HR results in positive feedbacks that enhance the net uptake of mineral nitrogen.

[67] In this study, we have analyzed the dynamics under the assumption that both soil and vegetation structure remain unaltered in the long term. This assumption has allowed us to simplify the inherent complexity associated with these systems and focus on the below-ground interaction of water, carbon, and nitrogen under different plant species composition. However, the results obtained in this study may be affected by this assumption and further research must be performed to incorporate the coevolutionary dynamics between soil structure and carbon and nitrogen.

[68] Although the numerical model implemented in this study simplifies many of the complex interactions found in natural ecosystems, it established that the passive movement of water in the subsurface by plant roots is an important mechanism that influences the below-ground biogeochemical dynamics and should be considered in the analysis of carbon and nitrogen processes that occur in natural ecosystems. This mechanism may be an important element in the understanding of current and long-term

biogeochemical patterns observed in experimental observations as well as an important variable that should be considered in climate change studies.

[69] **Acknowledgments.** This research has been funded by NSF grant ATM 06-28687 EAR 09-11205, and University of Illinois Dissertation Completion Fellowship. D.T.D. was also supported by the National Science Foundation's International Research Fellowship Program (IRFP), award OISE-0900556. D.T.D. also acknowledges support of the Jet Propulsion Laboratory, California Institute of Technology, under a contract with the National Aeronautics and Space Administration.

## References

- Aanderud, Z. T., and J. H. Richards (2009), Hydraulic redistribution may stimulate decomposition, *Biogeochemistry*, 95(2-3), 323-333, doi:10.1007/s10533-009-9339-3.
- Amenu, G. G., and P. Kumar (2008), A model for hydraulic redistribution incorporating coupled soil-root moisture transport, *Hydrol. Earth Syst. Sci.*, 12(1), 100, 55-74.
- Andren, O. (1992), Modelling the effects of moisture on barley straw and root decomposition in the field, *Soil Biol. Biochem.*, 24(8), 727-736, doi:10.1016/0038-0717(92)90246-T.
- Armas, C., J. H. Kim, T. M. Bleby, and R. B. Jackson (2011), The effect of hydraulic lift on organic matter decomposition, soil nitrogen cycling, and nitrogen acquisition by a grass species., *Oecologia*, 168, 11-22.
- Bird, J. A., and M. S. Torn (2006), Fine roots vs. needles: A Comparison of <sup>13</sup>C and <sup>15</sup>N dynamics in a Ponderosa Pine Forest Soil, *Biogeochemistry*, 79(3), 361-382, doi:10.1007/s10533-005-5632-y.
- Black, T. A., and J. Harden (1995), Effect of timber harvest on soil carbon at Blodgett experimental forest, California, *Can. J. For. Res.*, 25, 1385-1396.
- Bouvier-Brown, N. (2008), *Quantifying Reactive Biogenic Volatile Organic Compounds: Implications for Gas- and Particle-Phase Atmospheric Chemistry*, Univ. of Calif., Berkeley.
- Braakhekke, M. C., C. Beer, M. R. Hoosbeek, M. Reichstein, B. Kruijt, M. Schrumpf, and P. Kabat (2011), SOMPROF: A vertically explicit soil organic matter model, *Ecol. Modell.*, 222(10), 1712-1730, doi:10.1016/j.ecolmodel.2011.02.015.
- Brooks, J. R., F. C. Meinzer, R. Coulombe, and J. Gregg (2002), Hydraulic redistribution of soil water during summer drought in two contrasting pacific northwest coniferous forest, *Tree Physiol.*, 22, 1107-1117.
- Brooks, J. R., F. C. Meinzer, J. M. Warren, J. C. Domec, and R. Coulombe (2006), Hydraulic redistribution in a Douglas-fir forest: Lessons from system manipulations, *Plant Cell Environ.*, 29(1), 138-150.
- Burgess, S. S. O., M. A. Adams, N. C. Turner, and C. K. Ong (1998), The redistribution of soil water by tree root systems, *Oecologia*, 115(3), 306-311.
- Burgess, S. S. O., J. S. Pate, M. A. Adams, and T. E. Dawson (2000), Seasonal water acquisition and redistribution in the Australian woody phreatophyte, banksia prionotes, *Ann. Bot.*, 85(2), 215-224.
- Burgess, S. S. O., M. A. Adams, N. C. Turner, D. A. White, and C. K. Ong (2001), Tree roots: Conduits for deep recharge of soil water, *Oecologia*, 126(2), 158-165.
- Caldwell, M. M., and J. H. Manwaring (1994), Hydraulic lift and soil nutrient heterogeneity, *Nat. Resour. Res.*, 42, 321-330.
- Caldwell, M. M., and J. H. Richards (1989), Hydraulic lift—Water efflux from upper roots improves effectiveness of water-uptake by deep roots, *Oecologia*, 79(1), 1-5.
- Caldwell, M. M., T. E. Dawson, and J. H. Richards (1998), Hydraulic lift: Consequences of water efflux from the roots of plants, *Oecologia*, 113(2), 151-161.
- Dam, D., E. Veldkamp, and N. V. Breemen (1997), Soil organic carbon dynamics: Variability with depth in forested and deforested soils under pasture in Costa Rica, *Biogeochemistry*, 39(3), 343-375.
- Dawson, T. E. (1993), Hydraulic lift and water use by plants, Implications for water balance, performance and plant-plant interactions, *Oecologia*, 95(4), 565-574.
- de Kroon, H., E. van der Zalm, J. W. A. van Rheenen, A. van Dijk, and R. Kreulen (1998), The interaction between water and nitrogen translocation in a rhizomatous sedge (*Carex flacca*), *Oecologia*, 116(1-2), 38-49, doi:10.1007/s004420050561.
- D'Odorico, P., F. Laio, A. Porporato, and I. Rodriguez-Iturbe (2003), Hydrologic controls on soil carbon and nitrogen cycles, ii, a case study, *Adv. Water Resour.*, 26(1), 59-70.
- Domec, J. C., J. M. Warren, F. C. Meinzer, J. R. Brooks, and R. Coulombe (2004), Native root xylem embolism and stomatal closure in stands of douglas-fir and ponderosa pine: Mitigation by hydraulic redistribution, *Oecologia*, 141(1), 7-16.
- Drewry, D. T., P. Kumar, S. Long, C. Bernacchi, X.-Z. Liang, and M. Sivalapan (2010a), Ecohydrological responses of dense canopies to environmental variability: 1. Interplay between vertical structure and photosynthetic pathway, *J. Geophys. Res.*, 115, G04022, doi:10.1029/2010JG001340.
- Drewry, D. T., P. Kumar, S. Long, C. Bernacchi, X.-Z. Liang, and M. Sivalapan (2010b), Ecohydrological responses of dense canopies to environmental variability: 2. Role of acclimation under elevated CO<sub>2</sub>, *J. Geophys. Res.*, 115, G04023, doi:10.1029/2010JG001341.
- Egerton-Warburton, L. M., J. I. Querejeta, and M. F. Allen (2008), Efflux of hydraulically lifted water from mycorrhizal fungal hyphae during imposed drought, *Plant Signaling Behavior*, 3(1), 68-71.
- Elzein, A., and J. Balesdent (1995), Mechanistic simulation of vertical distribution of carbon concentrations and residence times in soils, *Soil Sci. Soc. Am. J.*, 59(5), 1328-1335.
- Espeleta, J. F., J. B. West, and L. A. Donovan (2004), Species-specific patterns of hydraulic lift in co-occurring adult trees and grasses in a sandhill community, *Oecologia*, 138(3), 341-349.
- Fierer, N., J. P. Schimel, and P. A. Holden (2003), Variations in microbial community composition through two soil depth profiles, *Microbiology*, 35, 167-176.
- Fisher, J. B., T. A. DeBiase, Y. Qi, M. Xu, and A. H. Goldstein (2005), Evapotranspiration models compared on a Sierra Nevada forest ecosystem, *Environ. Modell. Software*, 20(6), 783-796, doi:10.1016/j.envsoft.2004.04.009.
- Goldstein, A. H., N. E. Hultman, J. M. Fracheboud, M. R. Bauer, J. A. Panek, M. Xu, Y. Qi, A. B. Guenther, and W. Baugh (2000), Effects of climate variability on the carbon dioxide, water, and sensible heat fluxes above a ponderosa pine plantation in the sierra nevada (ca), *Agric. For. Meteorol.*, 101(2-3), 113-129.
- Hawkins, H.-J., H. Hettasch, A. G. West, and M. D. Cramer (2009), Hydraulic redistribution by protea "sylvia" (proteaceae) facilitates soil water replenishment and water acquisition by an understory grass and shrub, *Funct. Plant Biol.*, 36(8), 752-760.
- Hobbie, S. E. (1992), Effects of plant species on nutrient cycling, *Trends Ecol. Evol.*, 7(10), 336-339, doi:10.1016/0169-5347(92)90126-V.
- Horton, J. L., and S. C. Hart (1998), ecosystem process, *Science*, 13(6), 232-235.
- Hultine, K. R., W. L. Cable, S. S. O. Burgess, and D. G. Williams (2003), Hydraulic redistribution by deep roots of a Chihuahuan desert phreatophyte, *Tree Physiol.*, 23(5), 353-360.
- Ishikawa, C. M., and C. S. Bledsoe (2000), Seasonal and diurnal patterns of soil water potential in the rhizosphere of blue oaks: Evidence for hydraulic lift, *Oecologia*, 125, 459-465.
- Ivanov, V. Y., R. L. Bras, and D. C. Curtis (2007), A weather generator for hydrological, ecological, and agricultural applications, *Water Resour. Res.*, 43, W10406, doi:10.1029/2006WR005364.
- Jackson, R. B., H. A. Mooney, and E. D. Schulze (1997), A global budget for fine root biomass, surface area, and nutrient contents, *Proc. Natl. Acad. Sci. U. S. A.*, 94(14), 7362-7366.
- Jackson, R. B., J. S. Sperry, and T. E. Dawson (2000), Root water uptake and transport: Using physiological processes in global predictions, *Trends Plant Sci.*, 5(11), 482-488.
- Jobbágy, E. G., and R. B. Jackson (2000), The vertical distribution of soil organic carbon and its relation to climate and vegetation, *Ecol. Appl.*, 10(2), 423-436, doi:10.1890/1051-0761(2000)010[0423:TVDOSO]2.0.CO;2.
- Kaste, J. M., A. M. Heimsath, and B. C. Bostick (2007), Short-term soil mixing quantified with fallout radionuclides, *Geology*, 35(3), 243-246.
- Kätterer, T., M. Reichstein, O. Andren, and A. Lomander (1998), Temperature dependence of organic matter decomposition: A critical review using literature data analyzed with different models, *Biol. Fert. Soils*, 27(3), 258-262.
- Kieft, T. L., P. S. Amy, F. J. Brockman, J. K. Fredrickson, B. N. Bjornstad, and L. L. Rosacker (1993), Microbial abundance and activities in relation to water potential in the vadose zones of arid and semiarid sites, *Microbial Ecol.*, 26(1), 59-78.
- Liste, H.-H., and J. C. White (2008), Plant hydraulic lift of soil water—Implications for crop production and land restoration, *Plant Soil*, 313(1-2), 1-17.
- Ludwig, F., T. E. Dawson, H. Kroon, F. Berendse, and H. H. T. Prins (2003), Hydraulic lift in acacia tortilis trees on an east African savanna, *Oecologia*, 134(3), 293-300.



- Lundquist, E. J., K. M. Scow, L. E. Jackson, S. L. Uesugi, and C. R. Johnson (1999), Rapid response of soil microbial communities from conventional, low input, and organic farming systems to a wet/dry cycle, *Soil Biol. Biochem.*, 31(12), 1661–1675.
- Manzoni, S., and A. Porporato (2007), A theoretical analysis of nonlinearities and feedbacks in soil carbon and nitrogen cycles, *Soil Biol. Biochem.*, 39(7), 1542–1556, doi:10.1016/j.soilbio.2007.01.006.
- Manzoni, S., and A. Porporato (2009), Soil carbon and nitrogen mineralization: Theory and models across scales, *Soil Biol. Biochem.*, 41(7), 1355–1379, doi:10.1016/j.soilbio.2009.02.031.
- Matzner, S. L., and J. H. Richards (1996), Sagebrush (*Artemisia tridentata* Nutt.) roots maintain nutrient uptake capacity under water stress, *J. Exp. Bot.*, 47(8), 1045–1056, doi:10.1093/jxb/47.8.1045.
- McCulley, R. L., E. G. Jobbágy, W. T. Pockman, and R. B. Jackson (2004), Nutrient uptake as a contributing explanation for deep rooting in arid and semi-arid ecosystems, *Oecologia*, 141(4), 620–628, doi:10.1007/s00442-004-1687-z.
- Misson, L., J. A. Panek, and A. H. Goldstein (2004), A comparison of three approaches to modeling leaf gas exchange in annually drought-stressed ponderosa pine forests, *Tree Physiol.*, 24(5), 529–541.
- Misson, L., J. W. Tang, M. Xu, M. McKay, and A. Goldstein (2007), Influences of recovery from clear-cut, climate variability, and thinning on the carbon balance of a young ponderosa pine plantation, *Agric. Forest Meteorol.*, 130(3–4), 207–222, doi:10.1016/j.agrformet.2005.04.001.
- Misson, L., K. P. Tu, R. A. Boniello, and A. H. Goldstein (2006), Seasonality of photosynthetic parameters in a multi-specific and vertically complex forest ecosystem in the sierra nevada of california, *Tree Physiol.*, 26(6), 729–741.
- Nadezhkina, N., T. S. David, J. S. David, M. I. Ferreira, M. Dohnal, M. Tesa, K. Gartner, E. Leitgeb, and V. Nadezhdin (2010), Trees never rest: The multiple facets of hydraulic redistribution, *Library*, 444, 431–444, doi:10.1002/eco.
- Nye, P., and P. Tinker (1977), *Solute Movement in the Soil-Root System*, Blackwell Sci., University of California Press, Berkeley, Calif.
- Panek, J. A. (2004), Ozone uptake, water loss and carbon exchange dynamics in annually drought-stressed *Pinus ponderosa* forests: Measured trends and parameters for uptake modeling, *Tree Physiol.*, 24(3), 277–290.
- Porporato, A., P. D'Odorico, F. Laio, and I. Rodriguez-Iturbe (2003), Hydrologic controls on soil carbon and nitrogen cycles, i, modeling scheme, *Adv. Water Resour. Res.*, 26(1), 45–58.
- Querejeta, J., L. Egerton-Warburton, and M. Allen (2007), Hydraulic lift may buffer rhizosphere hyphae against the negative effects of severe soil drying in a California Oak savanna, *Soil Biol. Biochem.*, 39(2), 409–417, doi:10.1016/j.soilbio.2006.08.008.
- Querejeta, J. I., L. M. Egerton-Warburton, and M. F. Allen (2003), Direct nocturnal water transfer from oaks to their mycorrhizal symbionts during severe soil drying, *Oecologia*, 134(1), 55–64, doi:10.1007/s00442-002-1078-2.
- Quijano, J. C., P. Kumar, D. T. Drewry, A. Goldstein, and L. Misson (2012), Competitive and mutualistic dependencies in multispecies vegetation dynamics enabled by hydraulic redistribution, *Water Resour. Res.*, 48(5), doi:10.1029/2011WR011416.
- Richards, J. H., and M. M. Caldwell (1987), Hydraulic lift - substantial nocturnal water transport between soil layers by *Artemisia tridentata* roots, *Oecologia*, 73(4), 486–489.
- Richter, D. D., D. Markewitz, S. E. Trumbore, and C. G. Wells (1999), Rapid accumulation and turnover of soil carbon in a re-establishing forest, *Ecosystems*, 400, 14–16.
- Ryel, R. J., M. M. Caldwell, C. K. Yoder, D. Or, and A. J. Leffler (2002), Hydraulic redistribution in a stand of *Artemisia tridentata*: Evaluation of benefits to transpiration assessed with a simulation model, *Oecologia*, 130(2), 173–184, doi:10.1007/s004420100794.
- Schulze, E. D., M. M. Caldwell, J. Canadell, H. A. Mooney, R. B. Jackson, D. Parson, R. Scholes, O. E. Sala, and P. Trimbore (1998), Downward flux of water through roots (i.e. inverse hydraulic lift) in dry Kalahari sands, *Oecologia*, 115(4), 460–462.
- Scott, R. L., W. L. Cable, and K. R. Hultine (2008), The ecohydrologic significance of hydraulic redistribution in a semiarid savanna, *Water Resour. Res.*, 44, W02440, doi:10.1029/2007WR006149.
- Smith, D. M., N. A. Jackson, J. M. Roberts, and C. K. Ong (1999), Reverse flow of sap in tree roots and downward siphoning of water by *Grevillea robusta*, *Funct. Ecol.*, 13(2), 256–264.
- Stephens, S. L., and J. J. Moghaddas (2005), Fuel treatment effects on snags and coarse woody debris in a sierra nevada mixed conifer forest, *Forest Ecol. Manage.*, 214(1–3), 53–64, doi:10.1016/j.foreco.2005.03.055.
- Sylvia, D. M., J. J. Fuhrmann, P. G. Hartel, and D. A. Zuberer (2005), *Principles and Applications of Soil Microbiology*, pp. 369–388, Prentice Hall, Pearson, doi:10.1007/s10021.
- Vitousek, P. M., and P. A. Matson (1984), Mechanisms of nitrogen retention in forest ecosystems: A field experiment, *Science*, 225(4657), 51–52, doi:10.1126/science.225.4657.51.
- Walker, A. R. F., W. Cheng, and D. W. Johnson (2010), Mycorrhization of Ponderosa Pine in a second-growth Sierra Nevada Forest, *West. North Am. Nat.*, 70(1), 1–8.
- Warren, J. M., J. R. Brooks, F. C. Meinzer, and J. L. Eberhart (2008), Hydraulic redistribution of water from *Pinus ponderosa* trees to seedlings: Evidence for an ectomycorrhizal pathway, *New Phytol.*, 178(2), 382–394, doi:10.1111/j.1469-8137.2008.02377.x.
- Xu, M., and Y. Qi (2001), Soil-surface CO<sub>2</sub> efflux and its spatial and temporal variations in a young ponderosa pine plantation in northern california, *Global Change Biol.*, 7(6), 667–677.
- Zogg, G. P., D. R. Zak, D. B. Ringelberg, N. W. Macdonald, K. S. Pregitzer, and D. C. White (1997), Compositional and functional shifts in microbial communities due to soil warming, *Soil Sci. Soc. Am. J.*, 61(2), 475–481.